Organic Geochemistry 128 (2019) 94–107

Contents lists available at ScienceDirect

Organic Geochemistry

journal homepage: www.elsevier.com/locate/orggeochem

Sedimentary *n*-alkanes and *n*-alkanoic acids in a temperate bog are biased toward woody plants

Erika J. Freimuth [a,*], Aaron F. Diefendorf [a], Thomas V. Lowell [a], Gregory C. Wiles [b]

[a] Department of Geology, University of Cincinnati, Cincinnati, OH 45221, USA
[b] Department of Geology, The College of Wooster, Wooster, OH 44691, USA

ARTICLE INFO

Article history:
Received 7 September 2018
Received in revised form 28 December 2018
Accepted 13 January 2019
Available online 17 January 2019

Keywords:
Paleohydrology
Leaf wax
Hydrogen isotope
Apparent fractionation

ABSTRACT

Sedimentary plant waxes and their hydrogen and carbon (δ^2H and $\delta^{13}C$) isotopes are important proxies for past hydrologic and vegetation change. However sedimentary waxes accumulate from diverse sources, integrating uncertainties from: (i) variable isotope fractionation among plant species, and (ii) unresolved processes controlling the transport of waxes from plants to sediments. We address these uncertainties by comparing the molecular and isotopic composition of *n*-alkanes and *n*-alkanoic acids in recent bog sediments with all major plant species growing in the catchment of Browns Lake Bog (BLB) in Ohio, USA. There are two distinct plant assemblages at BLB, including a forest dominated by trees and a bog shoreline composed of shrubs, woody groundcover, herbs and graminoids. *n*-Alkane concentrations in trees were 10–300 times higher than in shoreline plants, while *n*-alkanoic acid concentrations were generally lower and comparable across all species. The overall range of wax δ^2H values among individual plants (77‰ for *n*-C_{29} alkane and 84‰ for *n*-C_{28} alkanoic acid) was likely driven by interspecies differences in biosynthetic δ^2H fractionation as well as source water differences between forest and shoreline plants. A considerably smaller range of δ^2H_{wax} values in the bog sediments (9‰ for *n*-C_{29} alkane and 11‰ for *n*-C_{28} alkanoic acid) suggests that sediments are either biased toward specific plants, or that signal averaging processes during or after deposition are constant. The combined δ^2H and $\delta^{13}C$ signatures of plant sources and sediments indicate a sediment bias mainly toward trees, with contributions from woody shrubs and groundcover growing in the bog shoreline. Within trees and woody shrubs, we observed δ^2H_{wax}–$\delta^{13}C_{wax}$ relationships of opposite sign for *n*-C_{29} alkane and *n*-C_{28} alkanoic acid, which we speculate may reflect contrasting seasonal timing of synthesis and plant metabolic status between compound classes. The net apparent δ^2H fractionation between precipitation and wax (ε_{app}) was approximately 30‰ larger for *n*-alkanes (−133‰) than for *n*-alkanoic acids (−103‰), both at the plant level and in sediments. These results demonstrate the sensitivity of sediments in a hydrologically closed basin to woody plants growing in the associated catchment and can guide ε_{app} estimates for sedimentary records from similar depositional settings.

1. Introduction

Plant waxes provide key records of past environmental conditions because they can retain their original molecular and isotopic composition when preserved in thermally immature sediments (Yang and Huang, 2003; Sessions et al., 2004; Schimmelmann et al., 2006; Diefendorf et al., 2015; Sessions, 2016). Different plant groups produce waxes with characteristic molecular distributions that can be used as indicators of plant growth environments (e.g., terrestrial or aquatic) or growth forms (e.g., tree, shrub, graminoid) that were dominant in the past (Eglinton and Hamilton, 1967; Ficken et al., 2000; Rommerskirchen et al., 2006; Aichner et al., 2010; Bush and McInerney, 2013; Freeman and Pancost, 2014). Additional paleoenvironmental information is contained in the stable carbon ($\delta^{13}C$) and hydrogen (δ^2H) isotopic composition of plant waxes. Plants using the C_3 photosynthetic pathway generally have smaller carbon isotope fractionation during wax biosynthesis than C_4 plants (Collister et al., 1994; Chikaraishi et al., 2004; Diefendorf and Freimuth, 2017). While there can be wide variability in lipid carbon isotope fractionation within and among species growing at the same location (e.g., Eley et al., 2016) or in the same biome (e.g., Diefendorf et al., 2010; Wu et al., 2017), the broad isotopic differences between photosynthetic pathways can be exploited to reconstruct the relative abundance of C_3 and C_4

* Corresponding author.
E-mail addresses: erika.freimuth@gmail.com, freimuej@mail.uc.edu (E.J. Freimuth).

https://doi.org/10.1016/j.orggeochem.2019.01.006
0146-6380/

vegetation in the past (Collins et al., 2013; Garcin et al., 2014; Tierney et al., 2017).

The hydrogen isotopic composition of precipitation (δ^2H_p) is the primary control on that of plant waxes (δ^2H_{wax}) both in modern plants (Sachse et al., 2006; Smith and Freeman, 2006; Feakins and Sessions, 2010; Tipple and Pagani, 2013) and in lake sediments (Sachse et al., 2004; Hou et al., 2008; Polissar and Freeman, 2010). Thus, δ^2H_{wax} in lacustrine (e.g., Tierney et al., 2008; Feakins et al., 2014; Rach et al., 2014) and marine (e.g., Pagani et al., 2006; Collins et al., 2013) sediments is commonly used to study past continental hydroclimate. Applications include constraining the onset and duration of past drying events (e.g., Rach et al., 2014) and reconstructing changes in moisture balance (e.g., Jacob et al., 2007) and the strength of monsoons (e.g., Bird et al., 2014). However, quantitative reconstruction of δ^2H_p using sedimentary δ^2H_{wax} is hindered by a limited understanding of: (1) the biological drivers of variable plant wax hydrogen isotope fractionation (ε_{app}) in plants, and (2) the mechanisms of leaf wax transport from plants to sediments and any associated biases in the preserved signal (Sachse et al., 2012). Together, these processes contribute a high degree of uncertainty in the application of sedimentary plant waxes, and therefore are the focus of this study.

1.1. Drivers of ε_{app} variability in living biomass

The primary relationship between δ^2H_p and δ^2H_{wax} is modified by secondary environmental and plant biological factors. These secondary factors include soil evaporation (McInerney et al., 2011) and leaf transpiration (Feakins and Sessions, 2010; Sachse et al., 2010; Kahmen et al., 2013a, 2013b), which can drive greater evaporative ^{2}H-enrichment of plant source water in more arid settings. Differences in plant physiology, leaf structure and rooting depth among plant groups can also lead to differences in the evaporative ^{2}H-enrichment of stem and leaf water (Smith and Freeman, 2006; Feakins and Sessions, 2010; Kahmen et al., 2013a, 2013b). In addition, all plants undergo a large (>100‰) negative biosynthetic fractionation (ε_{bio}) during lipid biosynthesis from intracellular water (Sachse et al., 2006, 2012). The cumulative result of these secondary factors is the net apparent fractionation (ε_{app}) between δ^2H_p and δ^2H_{wax}. Ultimately, estimates of ε_{app} are critical for plant wax paleohydrology because ε_{app} links measured δ^2H_{wax} to calculated δ^2H_p. However, because ε_{app} depends on the numerous contributing factors discussed above, it is subject to large uncertainties that hinder quantitative reconstructions of δ^2H_p. The total range in ε_{app} among species growing in the same location varies from 50‰ to 150‰ across temperate, tropical, arid, coastal and botanical garden environments (Hou et al., 2007b; Feakins and Sessions, 2010; Eley et al., 2014; Gao et al., 2014a; Cooper et al., 2015; Feakins et al., 2016). Large (>50‰) differences in ε_{app} among plants occupying the same growth environment complicates selection of accurate ε_{app} values for sedimentary leaf waxes, which accumulate from a mixture of plant sources at a single site. The underlying biological mechanisms for ε_{app} differences among plants at a single site are complex and include: phylogeny (due to contrasting leaf expansion patterns, leaf water ^{2}H-enrichment, and stored carbohydrate use in monocots and eudicots; McInerney et al., 2011; Kahmen et al., 2013b; Gao et al., 2014a); seasonality (with distinct periods of *n*-alkane synthesis among growth forms and taxonomic groups; Oakes and Hren, 2016); and possibly physiology (with lower stomatal conductance leading to wax ^{2}H-depeletion in conifers relative to angiosperms; Pedentchouk et al., 2008). In addition, different classes of *n*-alkyl lipids have been observed to have different ε_{app} values reflecting differences in biosynthetic fractionation (e.g., Chikaraishi and Naraoka, 2007; Hou et al., 2007b; Freimuth et al., 2017). This study includes both *n*-alkanes and *n*-alkanoic acids. While both compounds are commonly used in studies of past environments, *n*-alkanes are more widely studied in modern systems.

1.2. Leaf wax transfer from plant to sediment

The transport of leaf waxes from plant source to sediment sink is poorly understood and may bias the composition of sedimentary wax records (Pancost and Boot, 2004; Sachse et al., 2012; Nelson et al., 2018). There are three main mechanisms that deliver plant waxes to sediments: direct leaf fall, dry and wet deposition of aerosol particulate waxes, and transport of soil-derived waxes by rivers or overland flow (Diefendorf and Freimuth, 2017 and References therein). Each of these transport mechanisms operates on different temporal and spatial scales, potentially introducing bias toward different wax sources. For instance, leaf litter in temperate deciduous forests is highly localized and reflects the composition of adjacent trees (Burnham et al., 1992), while regional and long-range transport of aerosol waxes can integrate source areas on the order of hundreds to thousands of km (Conte et al., 2003; Nelson et al., 2017). The mix of transport pathways that ultimately dominate the wax flux in lake sediments can vary based on: vegetation assemblage in the source region (Gao et al., 2014b); catchment structure, including drainage area relief, the extent and composition of lowlands, and soil erosion by fluvial networks (Feakins et al., 2018); and the variable influence of atmospheric deposition, ranging from a minor (Meyers and Hites, 1982) to a major (>50%; Doskey, 2000) component of the total flux of terrestrial waxes to lake sediments in temperate North America. It is therefore critical to constrain the influence that plant wax sourcing and transport exert on the composition of plant wax records archived in sediments.

Plant wax transport is difficult to measure directly. Previous approaches have included the use of lake sediment traps (Daniels et al., 2017), suspended particulate matter filtering from rivers and lakes (Giri et al., 2015; van Bree et al., 2018) and high-volume air filters (Simoneit et al., 1977; Conte and Weber, 2002; Nelson et al., 2017) or rain collectors (Meyers and Hites, 1982). This study uses a dual-isotope approach to fingerprint the molecular and isotopic (δ^2H and $\delta^{13}C$) composition of *n*-alkanes and *n*-alkanoic acids in major wax sources (plants and particulate waxes) and associated sediments within a single catchment at Brown's Lake Bog (BLB), Ohio, USA.

This study site offers two main advantages. First, wax sourcing is simplified because the BLB catchment is relatively flat with no river or stream inputs, therefore the main wax sourcing mechanisms are simplified to direct leaf fall and atmospheric deposition, with no fluvial erosion of soils. Second, as a state nature preserve within an agricultural region, the BLB catchment has a unique distribution of plants. Within the property line, the site is dominated by deciduous forest, but with a distinct shoreline plant community surrounding the bog; outside the property line the region is dominated by C_4 corn (*Zea mays*). We use BLB to address the following questions: (1) How do leaf wax abundance and isotopic composition vary among species and growth forms at a single site?; (2) Are sedimentary plant waxes biased toward specific sources?; and (3) Do the molecular and isotopic compositions of two lipid classes (*n*-alkanes and *n*-alkanoic acids) differ at the plant and sediment level? Our approach extends beyond individual plants to examine the catchment-wide integration of plant waxes in sediments. Characterizing these integration mechanisms and associated sediment bias is a critical step in reducing the uncertainties in precipitation δ^2H reconstructions based on sedimentary plant waxes.

2. Materials and methods

2.1. Site description and sediment collection

BLB (40.6818°N, 82.0645°W; 291 m above sea level) is an ombrotrophic peatland on formerly glaciated terrain (Sanger and Crowl, 1979; Lutz et al., 2007; Glover et al., 2011). The bog includes a small open water area (288 m^2) surrounded by a shrub-dominated shoreline vegetation zone underlain by a *Sphagnum* moss mat (4329 m^2; Fig. 1). The bog and shoreline vegetation is set within a larger forest (370,496 m^2) which grades from a lowland deciduous fen into relatively well-drained oak-dominated kames (Fig. 1). The bog is hydrologically closed and is recharged by precipitation and groundwater. Bog water was collected approximately monthly during the 2014 and 2016 growing seasons using 30 ml Nalgene bottles. Precipitation was collected approximately monthly during the 2014 and 2015 growing seasons using 500 ml Nalgene bottles fitted with a funnel. A layer of mineral oil was used to prevent evaporation of collected precipitation. Approximately monthly, 12 ml of collected precipitation was transferred to an airtight exetainer vial and stored at 4 °C until isotope analysis.

The upper 1 m of sediment, including the sediment-water interface, was collected from the depositional center (2.5 m water depth) of BLB on January 25, 2015 using a Bolivian piston corer. The core was extruded in the field, transferred to Whirl-Pak bags at 1.0 cm increments, and kept frozen until lipid analysis. An additional 2 m Bolivian piston core was collected on January 30, 2016 and was used to constrain the age of the uppermost sediments using ^{210}Pb gamma counting on 22 samples from the upper 163 cm at the St. Croix Watershed Research Station, MN, USA (Supplementary Table S1). The same core was also used to determine magnetic susceptibility using a Barington MS2 meter in units of 10^{-7} m^3/kg, as well as percent total organic matter and total carbonate based on the mass loss on ignition after dried sediment (60 °C overnight) was baked at 550 °C (4 h) and 1000 °C (2 h), respectively (Heiri et al., 2001).

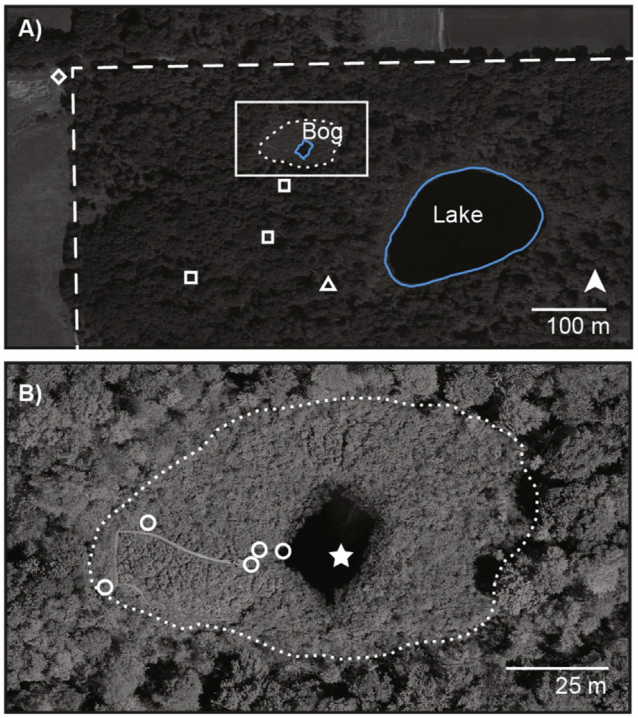

Fig. 1. Maps of Brown's Lake Bog (BLB) State Nature Preserve. Panel A shows the northwestern preserve boundary (dashed line), the bog and adjacent lake (blue lines), and sites of tree sampling (squares), *Z. mays* sampling (diamond) and precipitation collection (triangle). Note that the two southernmost squares (farthest from the bog) indicate the location of oak-dominated kames where *Q. alba* and *Q. rubra* trees were sampled. Panel B shows detail of the area inside the white box in panel A, including the bog shoreline vegetation zone (dotted line) with the locations of shoreline vegetation sampling (circles) and bog sediment collection (star). (For interpretation of the references to color in this figure legend, the reader is referred to the web version of this article.)

2.2. Plant sampling for lipid and stem water analysis

Leaves were collected from 20 species at BLB on September 20, 2015, including five deciduous angiosperm tree species (*Acer saccharinum*, *Prunus serotina*, *Quercus alba*, *Quercus rubra*, and *Ulmus americana*) that were previously sampled during the 2014 growing season (Freimuth et al., 2017). All trees were sampled in the forested area of BLB; the remaining 15 species were sampled in the bog shoreline zone (Fig. 1), and included woody shrubs (n = 2 species; *Toxicodendron vernix*, *Vaccinium corymbosum*), woody groundcover (n = 2 species; *Salix petiolaris*, *Vaccinium macrocarpon*), herbaceous plants (n = 7 species), C_3 graminoids (n = 3 species), and one moss (*Sphagnum* sp.). In addition, leaves from one C_4 graminoid (*Zea mays*, corn) were sampled from a farm bordering the BLB nature preserve to the west (Fig. 1). All leaves were collected in paper bags, frozen within 12 h of collection and freeze dried prior to lipid analysis (see Section 2.5).

An additional round of plant sampling was carried out on September 22, 2016 to assess variations in plant source water δ^2H. The same individual trees were resampled using an arborist's sling shot to remove one branch (<1.0 cm) from the uppermost canopy of each tree. The outer bark was immediately removed and each xylem sample was transferred to a pre-ashed glass exetainer vial, sealed with an airtight septa screwcap and kept in a dry cooler in the field. Xylem samples from woody bog plants were prepared the same way. Herbaceous bog plants were also stored in airtight exetainer vials, but the entire green stems were collected. All xylem samples were kept frozen (−20 °C) until water extraction.

2.3. Monitoring wet deposition of n-alkanes

Rain water was collected at BLB from July to December 2016 in order to quantify the flux of *n*-alkanes from aerosols via precipitation scavenging (e.g., Meyers and Hites, 1982; Gagosian and Peltzer, 1986). Two identical collectors were placed 5 m apart in a forest clearing with no overhead foliage within 200 m of the bog shoreline (Fig. 1). Each collector consisted of a solvent-rinsed 12 L glass carboy stabilized and shaded within a bucket buried approximately 30 cm into the ground. A 25.4 cm diameter funnel with internal and external mesh debris guards was fitted into the opening of each carboy to direct rainwater into the collector. The collectors were decanted monthly into solvent-rinsed glass bottles. Collected water was then filtered through ashed and pre-weighed glass fiber filters in the lab to collect particles >0.7 μm (Whatman GE, Little Chalfont, UK). Filters from each collector and sampling month were individually wrapped in combusted foil and stored at −20 °C until freeze drying prior to lipid extraction (see Section 2.5). After the final rainwater collection, each collector was solvent-rinsed with dichloromethane (DCM) and methanol (MeOH) to collect any residual lipids adsorbed to the carboy. These two samples were treated identically to the total lipid extract (TLE) from the filtered rainwater (see Section 2.5).

2.4. Xylem water extraction and δ^2H analysis

Xylem water was extracted using cryogenic vacuum distillation following the methods of West et al. (2006). Exetainer vials

containing frozen leaves and stems were evacuated to a pressure <8 Pa (<60 mTorr), isolated from the vacuum pump, and heated to 100 °C. Water vapor was collected in borosilicate test tubes immersed in liquid nitrogen for a minimum of 60 min. To verify extraction completion, samples were weighed following cryogenic vacuum distillation and then again after freeze drying. Based on the mass difference, the recovery of plant water was >95%. Collected water was thawed and pipetted into 2 ml crimp-top vials and refrigerated at 4 °C until analysis.

Analysis of xylem water δ^2H (δ^2H_{xw}) was made by headspace equilibration using 200 μl of water transferred to exetainer vials with a Pt catalyst added. Samples were purged using 2% H_2 in He for 10 min at 120 ml/min and equilibrated at 25 °C for 1 h. The isotopic composition of equilibrated headspace gas was analyzed on a Thermo Delta V Advantage isotope ratio mass spectrometer (IRMS) with a Thermo Gasbench II connected via a Conflo IV interface. Data were normalized to the VSMOW/SLAP scale using three in-house reference standards. Precision and accuracy based on independent standards were 3.4‰ (1σ, n = 13) and −0.48‰ (n = 5), respectively.

2.5. Lipid extraction, quantification and stable isotope analysis

Dry sediment and leaf samples were ground to a powder. Separate aliquots of the dry material were used for lipid extraction and bulk $\delta^{13}C$ analysis (see Section 2.6). Dried sediments and filtered rainwater samples (see Section 2.3) were solvent-extracted using an accelerated solvent extractor (ASE; Dionex 350) with 9:1 (v/v) DCM/MeOH with three extraction cycles at 100 °C and 10.3 MPa. For leaf lipid extraction, ~200 mg of powdered leaves was extracted by sonicating twice with 20 ml of DCM/MeOH (2:1, v/v), centrifuging and pipetting the lipid extract into a separate vial after each round of sonication.

For all samples, the TLE was dried under a gentle stream of nitrogen and base saponified to cleave fatty esters with 3 ml of 0.5 N KOH in MeOH/H_2O (3:1, v/v) for 2 h at 75 °C. Once cool, 2.5 ml of NaCl in water (5%, w/w) was added and acidified with 6 N HCl. The solution was extracted with hexanes/DCM (4:1, v/v), neutralized with $NaHCO_3$/H_2O (5%, w/w), and water was removed through addition of Na_2SO_4. Neutral and acid fractions were separated using DCM/isopropylalcohol (2:1, v/v) and 4% formic acid in diethyl ether, respectively, over aminopropyl-bonded silica gel. The neutral fraction was then separated into aliphatic and polar fractions using alumina gel column chromatography. The aliphatic fraction was separated over 5% silver impregnated silica gel with hexanes to collect saturated compounds. The acid fraction of sediment and leaf samples was evaporated under a gentle stream of nitrogen and methylated by adding ~1.5 ml of 95:5 MeOH/12 N HCl (v/v) of known δ^2H composition and heating at 70 °C for 12–18 h. HPLC grade water was added and fatty acid methyl esters (FAMEs) were extracted with hexanes and eluted through Na_2SO_4 to remove water before separation over 5% deactivated silica gel with DCM to collect FAMEs.

n-Alkanes and FAMEs were identified by GC–MS using an Agilent 7890A GC and Agilent 5975C quadrupole mass selective detector system and quantified using a flame ionization detector (FID). Compounds were separated on a fused silica column (Agilent J&W DB-5 ms) as the oven ramped from an initial temperature of 60 °C (held 1 min) to 320 °C (held 15 min) at 6 °C/min. Compounds were identified using authentic standards, fragmentation patterns and retention times. All samples were diluted in hexanes spiked with the internal standard 1,1′-binaphthyl at known concentration. Compound peak areas were normalized to those of 1,1′-binaphthyl and converted to concentration using response curves for an in-house mix of *n*-alkanes and FAMEs at a range of concentrations. Quantified concentrations were normalized to the dry mass of material extracted and are reported as μg wax/g dry leaf or dry sediment in Table 1. FAME concentrations were converted to equivalent *n*-alkanoic acid concentrations using respective molar masses. Average chain length (ACL) is the weighted average concentration of all the long-chain waxes, defined as:

$$ACL_{a-b} = \sum_{i=a}^{b} \frac{i[Ci]}{[Ci]} \quad (1)$$

where *a*–*b* is the range of chain lengths and C_i is the concentration of each wax compound with *i* carbon atoms. $ACL_{27\text{-}35}$ is used to indicate ACL values for *n*-C_{27} to *n*-C_{35} alkanes. $ACL_{26\text{-}30}$ is used to indicate ACL values for *n*-C_{26} to *n*-C_{30} alkanoic acids.

The isotopic compositions of *n*-alkanes and *n*-alkanoic acids were determined using a Thermo Trace GC Ultra coupled to an IRMS via a Conflo IV interface. The GC was connected to an Isolink pyrolysis reactor at 1420 °C for δ^2H analysis and an Isolink combustion reactor at 1000 °C for $\delta^{13}C$ analysis. The GC oven program ramped from 80 °C (held 2 min) to 320 °C (held 15 min) at a rate of 8 °C/min. For FAME analysis, samples and standards were run with the backflush valve open to exclude high-abundance compounds eluting before *n*-C_{22} alkanoic acid. A standard *n*-alkane mix of known δ^2H and $\delta^{13}C$ composition (Mix A5; A. Schimmelmann, Indiana University) was run every 6–8 samples and used to normalize the isotopic composition of samples to the VSMOW/SLAP scale for δ^2H and the Vienna Peedee Belemnite (VPDB) scale for $\delta^{13}C$ following Coplen et al. (2006). The δ^2H value of hydrogen added to *n*-alkanoic acids during derivatization was determined by mass balance of phthalic acid of known δ^2H composition (A. Schimmelmann, Indiana University) and derivatized methyl phthalate. The analytical uncertainty based on the pooled standard deviation from all replicate sample measurements was 3.0‰ and 4.4‰ for *n*-alkane and FAME δ^2H, respectively, and 0.3‰ for both *n*-alkane and FAME $\delta^{13}C$. The H_3^+ factor was tested daily during δ^2H analysis and averaged 6.2 ± 0.1 ppm mV^{-1}. Hydrogen isotopic fractionations (ε_{app}, ε_{bio}, etc.) are reported as enrichment factors (in units of per mil, ‰), using the following equation:

$$\varepsilon_{a-b} = \left[\frac{(\delta D_a + 1)}{(\delta D_b + 1)}\right] - 1 \quad (2)$$

where *a* is the product and *b* is the substrate.

2.6. Bulk foliar carbon isotope analysis

A separate aliquot of the powdered leaves was used to determine the $\delta^{13}C$ of bulk organic carbon. Bulk $\delta^{13}C$ analysis was performed via continuous flow (He; 120 ml/min) on a Costech elemental analyzer (EA) interfaced with a Thermo Delta V Advantage isotope ratio mass spectrometer (IRMS) via a Conflo IV. All $\delta^{13}C$ values were corrected for sample size dependency and normalized to the VPDB scale using a two-point calibration with in-house standards which were calibrated with IAEA standards (NBS-19, L-SVEC) to −38.26‰ and −11.35‰ VPDB following Coplen et al. (2006). Based on additional independent standards, sample precision was 0.03‰ (1σ, n = 11) and accuracy was 0.03‰ (1σ, n = 11). All data analyses were performed using JMP Pro 12.0 (SAS, Cary, NC, USA) and significance was attributed to alpha levels at or below 0.05.

3. Results

3.1. Environmental waters at BLB

Environmental and plant waters are reported in Fig. 2. Bog water δ^2H values increased steadily from March (−73‰) to May (−26‰), and remained relatively constant through autumn (May

Table 1
Mean *n*-alkane and *n*-alkanoic acid ACL and concentrations for plant species and forest litter (in μg/g dry leaf) as well as for the upper 40 cm of bog sediment (in μg/g dry sediment). Unidentified C_3 graminoid and herbaceous plant species are numbered with laboratory identifiers. Compounds that were not detected by GC–MS are indicated with n.d.

				n-Alkane (μg/g)					*n*-Alkanoic acid (μg/g)		
Species	Sample type	ACL_{27-35}	ACL_{26-30}	*n*-C_{27}	*n*-C_{29}	*n*-C_{31}	*n*-C_{33}	*n*-C_{35}	*n*-C_{26}	*n*-C_{28}	*n*-C_{30}
Bog sp. 3	C_3 Graminoid	30.0	28.5	2.3	11.0	12.3	2.1	n.d.	1.0	15.5	7.6
Rhynochospora capitellata	C_3 Graminoid	27.9	28.8	33.9	16.4	3.6	n.d.	n.d.	n.d.	10.0	6.6
Scirpus cyperinus	C_3 Graminoid	29.3	28.9	2.1	3.5	2.8	n.d.	n.d.	n.d.	7.3	6.5
Zea mays	C_4 Graminoid	31.4	29.0	2.6	14.3	26.6	23.8	6.0	n.d.	5.6	6.0
Bog sp. 5	Herb	28.8	29.3	0.3	2.4	n.d.	n.d.	n.d.	0.3	7.8	14.1
Bog sp. 6	Herb	28.9	29.0	4.1	23.1	4.6	n.d.	n.d.	9.7	35.2	63.9
Bog sp. 9	Herb	29.5	29.4	2.5	40.9	19.8	n.d.	n.d.	n.d.	3.7	8.9
Bog Ssp. 13	Herb	29.9	28.7	11.0	25.1	43.6	5.0	n.d.	1.1	32.0	18.5
Asclepias syriaca	Herb	28.5	28.9	5.2	7.4	1.4	n.d.	n.d.	n.d.	10.0	7.5
Peltandra virginica	Herb	27.8	28.6	6.4	4.1	n.d.	n.d.	n.d.	8.3	42.6	32.0
Sphagnum sp.	Herb	28.5	28.2	5.7	3.2	2.8	n.d.	n.d.	2.5	3.8	3.3
Toxicodendron vernix	Shrub	29.8	28.9	7.5	19.5	17.4	4.7	n.d.	2.4	14.7	17.9
Vaccinium corymbosum	Shrub	30.2	29.4	2.5	52.5	66.9	5.0	n.d.	0.2	8.9	23.3
Acer saccharinum	Tree	29.2	27.6	106.6	289.0	117.4	17.5	n.d.	33.5	34.4	17.2
Prunus serotina	Tree	31.0	27.3	16.9	731.0	1867.7	692.6	15.3	154.5	28.5	65.1
Quercus alba	Tree	28.7	27.6	28.7	34.1	13.7	1.6	n.d.	33.1	30.1	18.0
Quercus rubra	Tree	30.0	28.0	112.2	676.5	807.1	89.3	n.d.	71.3	36.3	30.5
Ulmus americana	Tree	29.3	27.2	6.3	64.3	15.0	1.4	n.d.	180.5	31.3	64.5
Salix petiolaris	Woody g.cover	28.6	28.9	6.4	11.9	2.3	n.d.	n.d.	1.0	12.7	12.6
Vaccinium macrocarpon	Woody g.cover	30.4	29.4	6.1	59.5	123.1	8.5	n.d.	n.d.	3.3	7.3
	Forest Litter	30.2	27.0	24.4	325.6	733.6	257.2	6.2	87.9	22.5	22.3
	Sediment	29.3	27.4	11.9	16.7	9.4	4.1	0.4	11.6	5.4	3.8

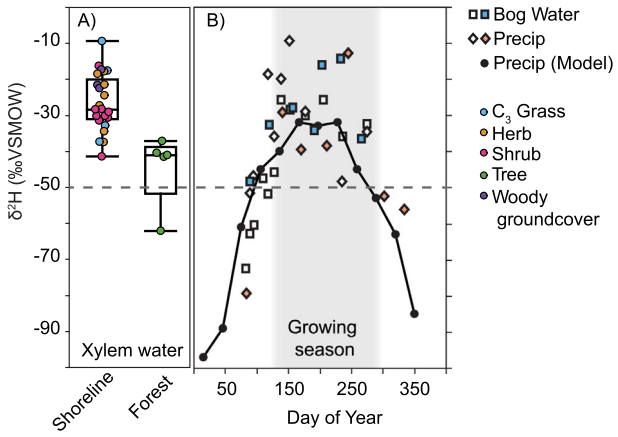

Fig. 2. The δ^2H values of plant xylem waters (A) and environmental waters (B) at BLB. Plant xylem waters were sampled in September 2016 from C_3 graminoids, herbs, shrubs and woody groundcover in the bog shoreline zone, as well as from trees in the forest. Bog water (squares) and precipitation (diamonds) are plotted by day of year (DOY) of collection in 2014 (white fill), 2015 (red fill) and 2016 (blue fill). The OIPC-modeled monthly and mean annual precipitation δ^2H values are indicated with black circles and the horizontal dashed line, respectively. The duration of the growing season (from bud break to leaf fall) is indicated by the shaded area. (For interpretation of the references to color in this figure legend, the reader is referred to the web version of this article.)

to October mean = −30 ± 4‰, n = 6). Precipitation collected approximately monthly during the 2105 growing season (March to November) ranged from −79‰ in March to −13‰ in September, with a mean of −44‰. The modeled annual mean δ^2H value for precipitation at BLB is −50 ± 2‰ from the Online Isotopes in Precipitation Calculator (OIPC; Welker, 2000; Bowen and Revenaugh, 2003; IAEA/WMO, 2015; Bowen, 2017). Plants growing in the bog shoreline zone had significantly higher δ^2H_{xw} values (−27 ± 8‰, n = 25) than trees occupying the forested zones of the catchment (−44 ± 10‰, n = 5; *t*-statistic = 0.0007, $p \leq 0.024$). There were no significant differences in δ^2H_{xw} values among shoreline plant growth forms (*t*-test, $p > 0.26$).

3.2. Leaf wax molecular and isotopic composition in plants

Leaf wax abundance varied widely among plant growth forms at BLB (Fig. 3; Table 1). We focus on *n*-C_{29} alkane and *n*-C_{28} alkanoic acid as chain-lengths generally indicative of terrestrial plants and commonly used in paleohydrology; additional chain-lengths are reported in Table 1 and Supplementary Table S2. Mean *n*-C_{29} alkane concentrations were an order of magnitude higher in trees (520 μg/g dry weight) than in the second most waxy growth form (shrubs, 31 μg/g). The lowest concentrations of *n*-C_{29} alkane were observed in herbs, C_3 graminoids and *Sphagnum* sp. growing in the bog shoreline (ranging from 1.8 to 8.6 μg/g). Within the tree growth form, *n*-C_{29} alkane concentrations were lowest in *Q. alba* and *U. americana* (34 and 64 μg/g), intermediate in *A. saccharinum* (289 μg/g) and highest in *Q. rubra* and *P. serotina* (676 and 731 μg/g). The ACL_{27-35} in all plants ranged from 28.8 in herbs to 31.4 in *Z. mays* (Fig. 4b), with comparable values in trees (29.6) and shrubs (29.9). Particulate waxes had similar ACL_{27-35} (29.5). By contrast, *n*-C_{28} acid concentrations and interspecies variability were considerably smaller, ranging from 4.0 μg/g in *Sphagnum* sp. to 33.8 μg/g in trees (Fig. 3a; Table 1). The ACL_{26-30} was consistently lower for trees (27.5) than for all other growth forms, which ranged from 28.7 in C_3 graminoid to 29.2 in shrubs and woody groundcover (Fig. 4).

Plant δ^2H_{wax} and $\delta^{13}C_{wax}$ values and sample n are reported in Table 3. The overall range in δ^2H_{wax} values among individual plants was 77‰ for *n*-C_{29} alkane and 84‰ for *n*-C_{28} alkanoic acid (Supplementary Table S2). Woody groundcover and C_3 graminoids had the lowest mean *n*-C_{29} alkane δ^2H values (−216‰ and −196‰, respectively). Mean *n*-C_{29} alkane δ^2H values were intermediate in shrubs, herbs and trees (−176‰, −167‰ and −163‰, respectively) and highest in the C_4 graminoid (*Z. mays*, −158‰; Table 3). C_3 graminoids had the lowest mean *n*-C_{28} acid δ^2H values (−182‰). Herbs

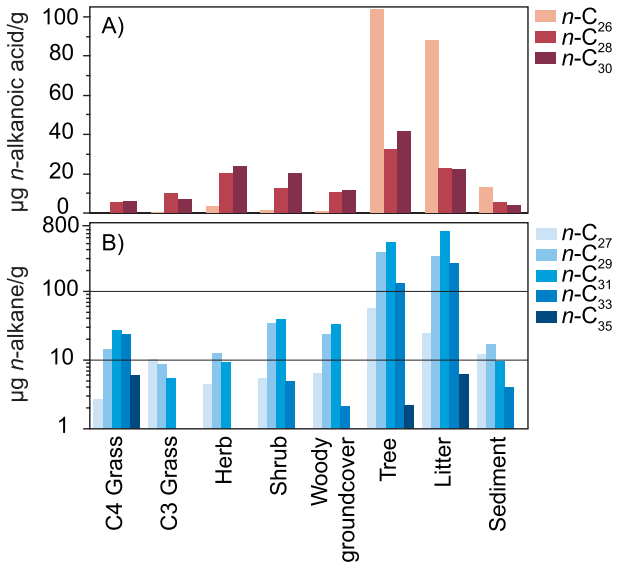

Fig. 3. Mean lipid abundance for each plant growth form, forest litter, and bog sediments at BLB, for: (A) n-C_{26} to n-C_{30} alkanoic acids, and (B) n-C_{27} to n-C_{35} alkanes, which are plotted on a log scale.

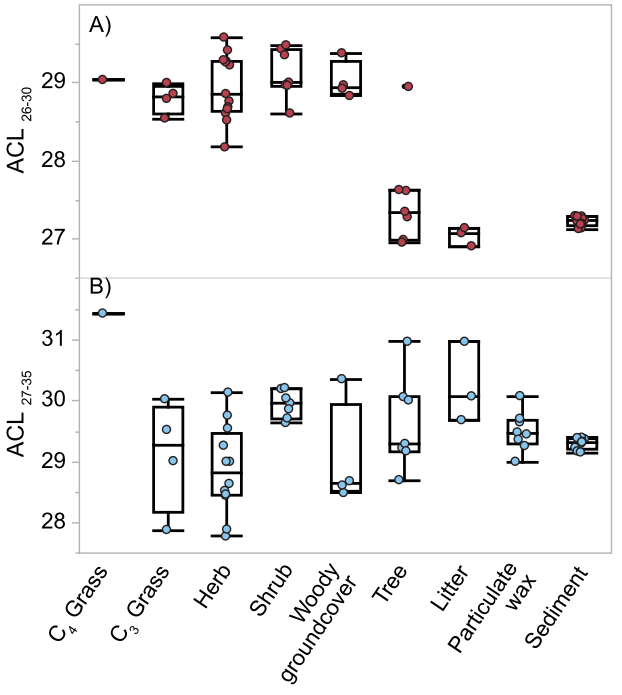

Fig. 4. Average chain length distributions for different plant growth forms, forest litter, rain-scavenged particulate aerosol waxes, and bog sediments at BLB, for: (A) n-alkanoic acids ($ACL_{26\text{-}30}$) and B) n-alkanes ($ACL_{27\text{-}35}$).

and shrubs had similar mean n-C_{28} acid δ^2H values (−153‰ and −152‰, respectively); trees were higher (−139‰); and *Z. mays* had the highest observed value (−101‰; Table 3). Prior studies have observed similar distributions, with δ^2H values for long-chain n-alkanes lowest in C_3 graminoids, highest in trees, and intermediate in herbaceous plants (Liu et al., 2006; Hou et al., 2007b; Eley et al., 2014; Cooper et al., 2015). Interspecies δ^2H_{wax} variability was 2–4 times greater for shoreline plants (n-C_{29} alkane and n-C_{28} alkanoic acid $1\sigma = 23‰$ and 17‰, respectively) than for trees in the forested areas of the catchment ($1\sigma = 6‰$ and 9‰, respectively).

Apparent δ^2H fractionation for n-C_{29} alkanes relative to mean annual precipitation δ^2H ($\varepsilon_{29/MAP}$) ranged among growth forms, from −175‰ in woody groundcover and −154‰ in C_3 graminoids to −133‰ in shrubs, −123‰ in herbs, and −119‰ in trees; $\varepsilon_{29/MAP}$ was smallest in *Z. mays* (−114‰; Table 3). The corresponding apparent fractionation for n-C_{28} alkanoic acid relative to mean annual precipitation δ^2H ($\varepsilon_{28/MAP}$) was approximately 15–55‰ smaller than $\varepsilon_{29/MAP}$ in each growth form, ranging from −139‰ in C_3 graminoids to −115‰ in woody groundcover, −108‰ in shrubs and herbs, −93‰ in trees and −54‰ in *Z. mays* (Table 3).

The overall range in leaf wax $\delta^{13}C$ values among individual plants was 21‰ for n-C_{29} alkane and 16‰ for n-C_{28} alkanoic acid (Supplementary Table S1). Interspecies n-C_{29} alkane $\delta^{13}C$ variability was higher for shoreline plants (2.5‰) than for trees (1.4‰). Isotopic variability in n-C_{28} alkanoic acid among species was comparable for shoreline plants and trees ($1\sigma = 2.4‰$ and 2.2‰, respectively). Mean n-C_{29} alkane $\delta^{13}C$ values were lowest in shoreline vegetation, ranging from herbs (−39.3‰) to C_3 graminoids (−36.3‰), woody groundcover (−35.7‰) and shrubs (−34.7‰). Trees had a higher mean n-C_{29} alkane $\delta^{13}C$ value (−33.8‰), and *Z. mays* was highest (−19.8‰), consistent with prior studies (Collister et al., 1994; Pancost and Boot, 2004; Chikaraishi and Naraoka, 2007). The distribution of $\delta^{13}C$ values by growth form was similar for n-C_{28} alkanoic acid, with the lowest mean values in herbs (−39.0‰), shrubs (−36.1‰) and C_3 graminoids (−35.5‰). Trees had a higher mean n-C_{28} alkanoic acid $\delta^{13}C$ value (−34.5‰), and *Z. mays* was highest (−24.5‰).

3.3. Particulate wax flux and composition

Due to relatively low lipid abundance, the particulate wax samples were only analyzed for n-alkanes and not for n-alkanoic acids. The apolar lipid fractions were dominated by n-C_{29} and n-C_{31} alkanes, with smaller amounts of n-C_{25}, n-C_{27} and n-C_{33} alkanes (Fig. 3b; Table 2). These molecular distributions are similar to those found previously in aerosols and precipitation and indicate that the long-chain ($\geq n$-C_{27}) alkanes are sourced primarily from terrestrial plants (Simoneit et al., 1977; Broddin et al., 1980; Meyers and Hites, 1982). The concentration of total n-alkanes (odd-carbon numbers from n-C_{23} to n-C_{31}) in precipitation at BLB ranged from 0.2 to 1.2 μg/L; n-C_{29} alkane ranged from 0.1 to 0.5 μg/L and n-C_{31} alkane ranged from 0 to 0.3 μg/L. These concentrations are comparable to, or smaller than, those found in rain and snow collected in the Midwestern USA, in which total n-alkane concentrations ranged from 0.4 to 8 μg/L (Meyers and Hites, 1982). Due to low abundance of monthly particulate wax samples collected at BLB, all monthly samples were combined to a single pooled sample prior to compound-specific isotope analysis. Pooled $\delta^{13}C$ values for particulate wax n-C_{29} and n-C_{31} alkanes were −30.7‰ and −31.1‰, more ^{13}C-enriched compared to most forest and bog shoreline plants (Fig. 5a). It is possible that the particulate wax was slightly ^{13}C-enriched relative to trees due to ablated waxes from the regionally dominant *Z. mays*, but such a contribution is likely small because particulate wax $\delta^{13}C$ values were ~10‰ lower than in *Z. mays* leaves. Further, the particulate wax $ACL_{27\text{-}35}$ closely matched forest and shoreline plants, significantly lower than in *Z. mays*. It was not possible to assess potential petrogenic contributions using the carbon preference index (CPI) because the abundance of even chain-length n-alkanes was below detection/quantitation limits in particulate wax samples. However, qualitatively, even chain-lengths were far less abundant than odd chain-lengths and therefore indicates a strong odd-over-even preference consistent with modern plant rather than petrogenic sources. Pooled δ^2H values for particulate wax n-C_{29} and n-C_{31} alkanes were −167‰ and −156‰, closely matching the n-C_{29} alkane values measured in trees and forest litter (Fig. 5a).

Table 2
Rain-scavenged particulate wax sampling dates with filtered rainwater volume, ACL, *n*-alkane concentration (in μg/liter of rainwater) and the $\delta^{13}C$ and $\delta^{2}H$ values for each sample. Residual samples were from solvent-rinsed carboys and the pooled data are for a single sample combined from all others (see Section 2.3). Compounds that were not detected by GC–MS are indicated with n.d.

					n-alkane concentration (μg/liter)						$\delta^{13}C$ *n*-alkane (‰)			$\delta^{2}H$ *n*-alkane (‰)		
Date Start	Date Stop	Collector	Filtered volume (liters)	ACL_{27-31}	*n*-C_{21}	*n*-C_{23}	*n*-C_{25}	*n*-C_{27}	*n*-C_{29}	*n*-C_{31}	*n*-C_{29}	*n*-C_{31}	*n*-C_{33}	*n*-C_{29}	*n*-C_{31}	*n*-C_{33}
7/22/16	8/20/16	A	1.6	29.7	0.24	0.24	n.d.	n.d.	0.33	0.18	−33.9	−33.9				
7/22/16	8/20/16	B	2.3	29.0	n.d.	n.d.	n.d.	n.d.	0.35	n.d.	−31.5					
8/20/16	9/22/16	A	4.3	29.5	n.d.	n.d.	n.d.	0.03	0.08	0.07						
8/20/16	9/22/16	B	3.4	30.1	n.d.	n.d.	n.d.	n.d.	0.08	0.09						
9/22/16	11/1/16	A	5.5	29.6	n.d.	n.d.	0.02	0.06	0.21	0.21	−32.0	−32.3				
9/22/16	11/1/16	B	10.8	29.5	n.d.	n.d.	n.d.	0.05	0.18	0.13	−31.7	−32.0				
11/1/16	12/31/16	A	4.0	29.4	n.d.	n.d.	0.06	0.15	0.42	0.31	−31.3	−30.7				
11/1/16	12/31/16	B	4.2	29.3	n.d.	0.11	0.09	0.19	0.50	0.32	−31.4	−31.4				
Residual		A	NA	29.5	n.d.	n.d.	0.36	0.91	2.75	2.27	−31.5	−31.4				
Residual		B	NA	29.6	n.d.	n.d.	n.d.	0.50	2.22	1.80	−31.9	−32.6				
Pooled											−30.8	−31.1	−30.0	−167	−156	−159.2

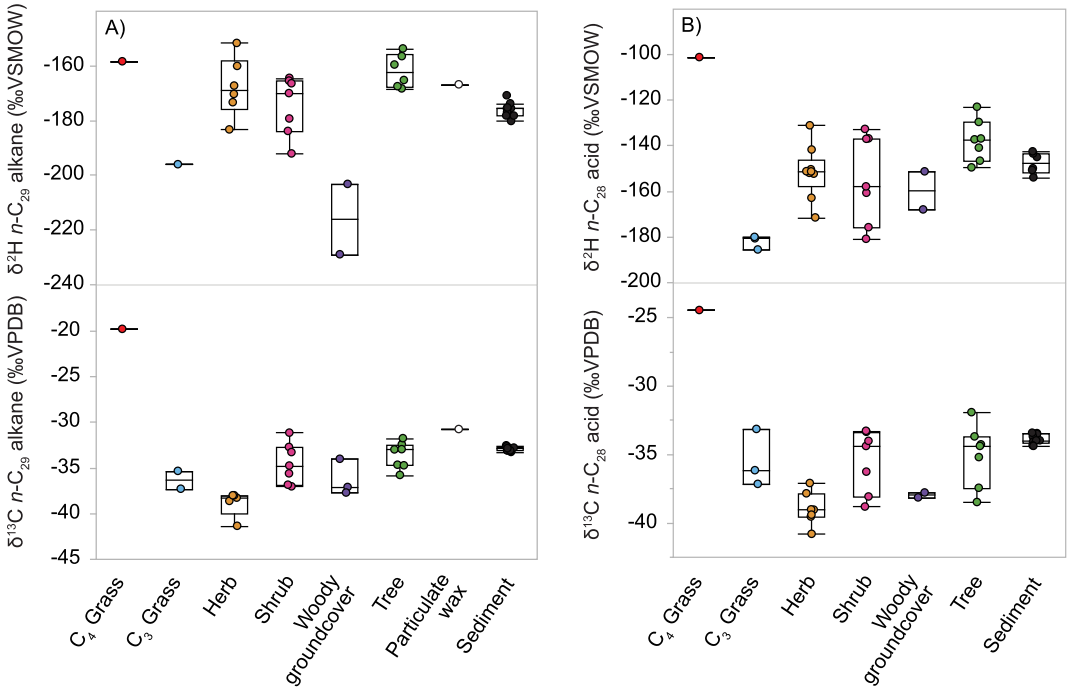

Fig. 5. The $\delta^{2}H$ and $\delta^{13}C$ composition of: (A) *n*-alkanes, and (B) *n*-alkanoic acids extracted from each plant growth form (C_4 grass is *Z. mays*), forest litter, rain-scavenged aerosols, and bog sediments at BLB.

3.4. Bog sediment chronology and bulk properties

Bog sediment chronology was established using ^{210}Pb on the core collected in 2016 with an oldest reliable date of 1848 ± 10 CE at 92.5 cm (Supplementary Table S2) and a mean sediment accumulation rate of 0.81 cm/yr since ~1900 CE. The sediment was uniformly fine-grained and dark brown over the entire collected interval. The magnetic susceptibility was $<6 \times 10^{-7}$ m^3/kg for most of the 0–40 cm interval, with the exception of an abrupt increase at 26 cm to 36×10^{-7} m^3/kg. From loss on ignition, the mean total organic content was 66% in the upper 24 cm, 87% from 26 to 32 cm, and 69% from 34 to 80 cm. Based on sediment chronology and bulk characteristics we limited our plant wax sampling strategy (Section 2.5) to the upper 40 cm of sediment, which corresponds to the years 1998–2015 CE. During this time, the vegetation assemblage and distribution within the BLB catchment would have been comparable to today because the site has remained a state nature preserve since 1967 CE.

3.5. Plant wax molecular and isotopic composition in bog sediments

The upper 40 cm of bog sediments contained plant waxes with a mean ACL_{27-35} of 29.3 and ACL_{26-30} of 27.4. The most abundant compound was generally the *n*-C_{29} alkane (17 μg/g dry sediment), followed by *n*-C_{27} and *n*-C_{31} alkanes (12 and 9 μg/g, respectively; Table 1). The mean CPI for *n*-alkanes and *n*-alkanoic acids in sediments (14.6 and 3.7, respectively; SupplementaryTable S2) were consistent with mean CPI for terrestrial plant sources (13.0 and 5.0, respectively; Supplementary Table S2; Freeman and Pancost, 2014). Long-chain *n*-alkanoic acids were dominated by the *n*-C_{26} alkanoic acid (12 μg/g). Average concentrations for *n*-C_{28} and *n*-C_{30} alkanoic acids were lower (5 and 4 μg/g, respectively; Table 1).

The total range in δ^2H_{wax} values for the upper 40 cm of sediments was 9‰ for *n*-C_{29} alkane and 11‰ for *n*-C_{28} alkanoic acid, with mean values of −176 ± 3‰ (n = 11) and −148 ± 5‰ (n = 6), respectively (Table 3). Corresponding $\varepsilon_{29/MAP}$ and $\varepsilon_{28/MAP}$ values in sediments were −133 ± 3‰ and −103 ± 5‰ (n = 6). The range in $\delta^{13}C_{wax}$ values in sediments was <1‰, with a mean of −32.9 ± 0.2‰ (n = 11) for *n*-C_{29} alkane and −33.9 ± 0.36‰ (n = 10) for *n*-C_{28} alkanoic acid. We cannot rule out lipid alteration or ongoing diagenesis in the relatively immature BLB sediments (Meyers et al., 1980). Over the 40 cm sediment profile, we observed a strong decrease in *n*-alkane CPI (from 24 to 7; n = 11, R^2 = 0.77, p = 0.0004), and a moderate increase in *n*-alkanoic acid CPI (from 3.5 to 4.9; n = 11, R^2 = 0.37, p = 0.05) with depth. Shifts in CPI with depth in soils and recent lake sediments have been attributed to degradation or microbial inputs (e.g., Cranwell, 1981; Meyers and Ishiwatari, 1993; Nguyen Tu et al., 2017). Importantly, there was no significant change in the $\delta^{13}C$ or δ^2H values for the *n*-C_{29} alkane (p = 0.12 and 0.16, respectively) or *n*-C_{28} alkanoic acid (p = 0.07 and 0.62, respectively) with depth in BLB sediments (Supplementary Table S2), consistent with a prior study that found stable *n*-alkane $\delta^{13}C$ values in plant litter over a comparable (23 yr) timespan (Huang et al., 1997). Therefore, while ongoing diagenesis may impact molecular distributions of sediments, these processes should not affect lipid isotopic comparisons with modern plants at BLB in the following discussion.

4. Discussion

4.1. Drivers of δ^2H_{wax} differences among plants

One major challenge for interpreting δ^2H_p from sedimentary δ^2H_{wax} is the wide range in ε_{app} values among plant species and growth forms, even those growing at the same site with the same hydroclimate conditions. The range in δ^2H values observed for *n*-C_{29} alkane (77‰) and *n*-C_{28} alkanoic acid (84‰) among all major plant species at BLB is comparable with that observed among diverse growth forms in other temperate ecosystems (75–98‰ and 100–194‰, respectively; Chikaraishi and Naraoka, 2007; Hou et al., 2007b; Eley et al., 2014; Cooper et al., 2015). One possible driver of the range in δ^2H_{wax} values observed at BLB is differences in source water used by plants growing in different zones of the catchment. Plants in the bog shoreline zone had δ^2H_{xw} values that reflected May to October bog water δ^2H values (−27‰ to −30‰; Fig. 2). The xylem water of shoreline plants was ^2H-enriched by 17‰ on average compared to trees, in which δ^2H_{xw} (−44‰) was closer to mean annual precipitation δ^2H (−50‰). In an earlier study, δ^2H_{xw} values in trees at BLB were relatively stable throughout the entire growing season (−50 ± 10‰ 1σ; n = 70; Freimuth et al., 2017). Therefore, September δ^2H_{xw} values reported here for trees should be comparable to source water used by trees during spring lipid synthesis.

We did not explore seasonal changes in δ^2H_{wax} of shoreline plants, and it is possible that the diverse species present in the shoreline zone synthesize wax at different (or multiple) points throughout the growing season (Pedentchouk et al., 2008; Sachse et al., 2009; Newberry et al., 2015). For instance, a shoreline plant producing leaf wax in March or April could be accessing bog water that is ^2H-depleted by ~20–30‰ compared to the relatively stable bog water values for the rest of the growing season (Fig. 2). Therefore, interspecies differences in the timing of leaf maturation and lipid synthesis may be factors contributing to the pronounced variability in δ^2H_{wax} values among shoreline species. However, seasonal changes in early spring bog water (~20–30‰) cannot account for the total range of δ^2H_{wax} values observed in shoreline plants.

The isotopic differences between the primary source water for shoreline plants (bog water) and trees (precipitation-fed soil water) may be amplified by physiological factors particular to the plants growing in different areas within the catchment. For instance, shoreline graminoids, herbs and shrubs generally have shallower rooting depths than the trees and may therefore access source water that is more evaporatively ^2H-enriched. Further, many shoreline plants at BLB grow on *Sphagnum* hummocks that are subaerially exposed and therefore more vulnerable to evaporative ^2H-enrichment than forest soils (Nichols et al., 2010), which are shielded from evaporation by canopy and groundcover. These factors, along with a greater diversity of growth forms, physiology and leaf morphologies in the shoreline zone, may contribute to the 2–4 times larger variability in *n*-C_{29} alkane among shoreline plants than among the tree species (Levene test, p = 0.04).

Nevertheless, differences in source water δ^2H cannot account for the overall range in δ^2H_{wax} values among plants. Species-level δ^2H_{xw} had no significant relationship with *n*-C_{29} alkane δ^2H (R^2 = 0.17, p = 0.08, n = 19), but could explain approximately one third of the variation in *n*-C_{28} alkanoic acid δ^2H (R^2 = 0.36, p = 0.002, n = 24). Therefore, differences in biosynthetic fractionation among species must account for the majority of the observed range in δ^2H_{wax} values among species sharing common growth conditions and similar source water. We did not analyze leaf water δ^2H values and therefore cannot approximate ε_{bio} for each species. However, in prior studies, $\varepsilon_{wax/leaf\ water}$ (an estimate of ε_{bio}) ranged by up to ~200‰ among species in a tropical forest (Feakins et al., 2016), and by up to ~150‰ among species in a temperate salt marsh (Eley et al., 2014), where the total range in plant xylem water (38‰) was comparable to that at BLB for multiple growth forms. Therefore, a wide range (>70‰) of biologically driven δ^2H_{wax} variability among species at a single site can be expected (e.g., Hou et al., 2007b; Eley et al., 2014), owing mainly to differences in ε_{bio}. While it is important to understand the specific drivers of ε_{app} variability in plants, the ultimate representation of this variability in sediments is most relevant to the application of the δ^2H_{wax} paleohydrology proxy. Identifying which plant sources, if any, are preferentially represented in sediments will help to inform ε_{app} estimations for interpretation sedimentary δ^2H_{wax} records.

4.2. Sediment bias toward n-alkane sources

Comparing the molecular and isotopic composition of plant waxes in vegetation with the associated sediments can help identify bias in the wax signal preserved in sediments. The total range in *n*-C_{29} alkane and *n*-C_{28} alkanoic acid δ^2H_{wax} values at BLB was far greater among plant species (77‰ and 84‰, respectively for each compound) than in bog surface sediments (9 and 11‰, respectively; Table 3; Fig. 5). Reduced variability in δ^2H_{wax} values at the sediment level indicates that the integration of plant waxes in sediments involves either consistent proportional mixing of major sources over the ~20 years of sediment accumulation represented, or biased incorporation of lipids from a subset of sources.

Terrestrial plant lipids are delivered to lacustrine sediments through three primary transport mechanisms: direct leaf fall, dry or wet deposition of particulate wax in aerosols or dust, and erosion of soil-derived waxes (Diefendorf and Freimuth, 2017). The latter process is likely minimal at BLB, as there are no surface water inputs to the hydrologically closed bog. Additionally, total relief at the site is low (12 m) and focused around several kames in the interior of the forest with extensive groundcover that acts to stabilize their soils. Therefore, the main modes of plant lipid transport to sediments at BLB are likely to be direct leaf fall and dry or wet deposition of particulate aerosol waxes.

In a simplified case, if sedimentary plant waxes at BLB were a mixture derived from leaves of all plant sources (ignoring

Table 3
Summary isotope data (mean, 1σ, n) for plant xylem water and wax δ^2H (‰ VSMOW) and $\delta^{13}C$ (‰ VPDB), with corresponding fractionation relative to xylem water ($\varepsilon_{wax/xw}$) and mean annual precipitation ($\varepsilon_{wax/MAP}$), by species. Mean data for each growth form, rain-scavenged particulate wax and bog sediments are in bold text.

			δ^2H *n*-alkane (‰)									δ^2H *n*-acid (‰)			$\delta^{13}C$ *n*-alkane (‰)						$\delta^{13}C$ *n*-acid (‰)			$\varepsilon_{wax/xw}$ (‰)			$\varepsilon_{wax/MAP}$ (‰)		
Species	Sample Type	δ^2H_{xw} (‰)	1σ	n	*n*-C_{29}	1σ	n	*n*-C_{31}	1σ	n	*n*-C_{28}	1σ	n	*n*-C_{29}	1σ	n	*n*-C_{31}	1σ	n	*n*-C_{28}	1σ	n	*n*-C_{29}	*n*-C_{31}	*n*-C_{28}	*n*-C_{29}	*n*-C_{31}	*n*-C_{28}
Bog Sp. 3	C3 Graminoid	−18		1							−186			−37.3			−37.7			−37.2					−171			−143
R. capitellata	C3 Graminoid	−9		1	−196						−181			−35.4			−36.0			−36.2			−189		−173	−154		−138
S. cyperinus	C3 Graminoid	−35	3	2							−180									−33.2					−150			−137
	C3 Graminoid	**−21**	**13**	**3**	**−196**						**−182**	**3**	**3**	**−36.3**	**1**	**2**	**−37**	**1**	**2**	**−35.5**	**2**	**3**	**−189**		**−165**	**−154**		**−139**
Z. mays	**C4 Graminoid**				**−158**			**−165**			**−101**			**−19.8**			**−20.0**			**−24.5**			**−158**	**−165**	**−101**	**−114**	**−121**	**−54**
Bog Sp. 5	Herb	−34		1							−162	14	2												−132			−118
Bog Sp. 6	Herb	−18		1	−160	11	2				−152	1	2	−38.2			−37.4			−39.0	0.01	2	−144		−137	−115		−107
Bog Sp. 9	Herb				−160			−151						−41.4			−42.2						−160	−151		−116	−107	
Bog Sp. 13	Herb				−178	7	2	−162	7	2	−141	14	2	−38.3	0.4	2	−39.3	0.4	2	−37.5	0.5	2	−178	−162	−141	−135	−118	−96
A. syriaca	Herb										−163									−39.4					−163			−119
P. virginica	Herb	−37		1	−170						−146	6	2							−40.2	0.9	2	−138		−113	−127		−101
Sphagnum sp.	Herb	−22	4	3																								
	Herb	**−28**	**9**	**4**	**−167**	**9**	**4**	**−157**	**7**	**2**	**−153**	**10**	**5**	**−39.3**	**2**	**3**	**−39.6**	**2**	**3**	**−39.0**	**1**	**4**	**−155**	**−157**	**−137**	**−123**	**−112**	**−108**
T. vernix	Shrub	−27	6	6	−167	2	4	−171	8	4	−169	11	4	−33.2	1.8	4	−34.1	1.8	4	−33.8	0.5	4	−143	−147	−146	−123	−127	−125
V. corymbosum	Shrub	−32	5	5	−185	6	3	−161	3	3	−136	2	3	−36.2	1.3	3	−38.1	0.9	3	−37.7	1.3	3	−158	−133	−107	−142	−117	−90
	Shrub	**−30**	**4**	**2**	**−176**	**13**	**2**	**−166**	**7**	**2**	**−152**	**24**	**2**	**−34.7**	**2**	**2**	**−36.1**	**3**	**2**	**−35.8**	**3**	**2**	**−151**	**−140**	**−126**	**−133**	**−122**	**−108**
A. saccharinum	Tree	−40			−168						−137			−34.7			−33.2			−33.7			−133		−101	−124		−92
P. serotina	Tree	−42			−160			−164			−150			−33.0			−32.6			−31.9			−123	−128	−113	−115	−120	−105
Q. alba	Tree	−41			−165						−137			−34.7			−35.3			−34.3			−130		−100	−121		−92
Q. rubra	Tree	−37			−155	2	2	−154	3	2	−144	4	2	−32.1	0.5	2	−33.8			−34.8	0.6	2	−123	−122	−111	−111	−110	−99
U. americana	Tree	−62			−168			−147			−126	5	2	−34.4	2.0	2	−33.6	1.5	2	−38.0	0.7	2	−113	−147	−98	−125	−102	−80
	Tree	**−44**	**10**	**5**	**−163**	**6**	**5**	**−155**	**9**	**3**	**−139**	**9**	**5**	**−33.8**	**1**	**5**	**−33.7**	**1**	**5**	**−34.5**	**2**	**5**	**−124**	**−132**	**−104**	**−119**	**−111**	**−93**
S. petiolaris	Woody g.cover	−22		1	−203						−160	12	2	−37.4	0.4	2	−39.6	0.5	2	−38.0	0.3	2	−185		−140	−161		−115
V. macrocarpon	Woody g.cover	−17			−229			−219						−34.0			−35.0						−216	−205		−188	−178	
	Woody g.cover	**−20**	**4**	**2**	**−216**	**18**	**2**	**−219**			**−160**			**−35.7**	**2**	**2**	**−37.3**	**3**	**2**	**−38.0**			**−200**	**−205**	**−140**	**−175**	**−178**	**−115**
	Particulate Wax				**−167**			**−156**						**−30.8**			**−31.1**									**−123**		
	Bog Sediment				**−176**	**3**	**10**	**−169**	**3**	**10**	**−148**	**5**	**6**	**−32.9**	**0.2**	**11**	**−32.8**	**0.2**	**11**	**−33.9**	**0.4**	**10**				**−133**	**−125**	**−103**

interspecies differences in leaf biomass production, relative abundance and spatial distribution on the landscape), then the expected δ^2H_{wax} and $\delta^{13}C_{wax}$ in sediments could be estimated using the concentration-weighted mean isotopic composition of all plant species. The concentration-weighted mean *n*-C_{29} alkane δ^2H and $\delta^{13}C$ from plants at BLB (−161‰ and −33.1‰, respectively; Fig. 6) is indistinguishable from sediment $\delta^{13}C$ (−32.9‰; *t*-test, $p = 0.88$), but significantly ^2H-enriched relative to sediment δ^2H (−176 ± 2.5‰; *t*-test, $p = 0.05$; Fig. 6). The concentration-weighted δ^2H_{wax} is likely ^2H-enriched compared to sediments because it is heavily weighted toward *P. serotina* and *Q. rubra* (−160‰ and −155‰, respectively), which had *n*-C_{29} alkane concentrations 2–50 times higher than all other trees, and 10–300 times higher than shoreline species. This indicates that sediments do not simply reflect the plants that produce the most wax, but instead are a complex mixture of sources, possibly modified by the relative abundance and leaf biomass production (which would favor trees; Fig. 1a) or spatial distribution (which would favor shoreline plants growing in close proximity to the bog; Fig. 1b) of species and growth forms. For *n*-C_{31} alkane, the discrepancy between the concentration-weighted mean δ^2H value for plants (−155‰) and that measured in sediments (−176‰) was even more pronounced, indicating that there must be significant sedimentary contributions from sources that are more ^2H-depleted than trees, but with a similar $\delta^{13}C$ value. This rules out significant contributions from the particulate waxes we measured, which had *n*-C_{29} to *n*-C_{33} alkanes that were consistently ^2H-enriched (by 9–13‰) and ^{13}C-enriched (by 1.7–3.3‰) relative to sediments (Fig. 6; Table 3 and Supplementary Table S2).

Likewise, significant contributions from *Z. mays* can be ruled out because its *n*-C_{29} alkane values were consistently enriched in both ^{13}C (by >10‰) and ^2H relative to sediments (Figs. 5 and 6; Table 3) and its ACL was also distinct from sediments (Fig. 4). We also consider that if waxes from *Z. mays* were transferred to sediments, direct leaf fall is not likely to be a dominant transport mechanism because of the plant's annual lifespan, the intervention of seasonal harvesting, and the wide forest buffer (150 m to 1 km) between the bog and adjacent agricultural fields (Fig. 1). Given the plant distribution and the lack of surface water as a mechanism for soil transport, the most likely mechanism to deliver wax from *Z. mays* to bog sediments is the deposition of particulate aerosols. Therefore, distinctly ^{13}C-enriched wax values in sediments may serve as an additional tracer for the contribution of particulate aerosol waxes. *Z. mays* had high *n*-C_{33} alkane concentrations relative to other plant sources so we compared the $\delta^{13}C$ values of *n*-C_{33} alkanes in sediments (−33.3 ± 0.5‰, 1σ) with rain-scavenged aerosol wax (−30‰) and *Z. mays* (−19.7‰). Both sources were ^{13}C-enriched by more than 2σ of the mean $\delta^{13}C_{wax}$ in sediments, indicating that despite the prevalence of agricultural *Z. mays* at the regional scale, its distinct $\delta^{13}C_{wax}$ composition is not reflected in BLB sediments, which likely reflect a more localized signal from the leaves of surrounding vegetation. A minor contribution of particulate waxes to sediments at BLB is consistent with recent evidence from a temperate forested region in Europe where the dry deposition of particulate waxes was estimated to contribute ~20% of the total wax flux to sediments (Nelson et al., 2017, 2018).

Based on the limited contribution of particulate sources, we excluded the particulate wax and *Z. mays* data when comparing all of the sediment and species-level *n*-alkane isotope data using the Stable Isotope Mixing Models in R (simmr) package (Parnell et al., 2010, 2013; Parnell, 2016; R Core Team, 2017; Supplementary Table S3). This dual-isotope mixing model uses summary (mean ± 1σ) δ^2H_{wax} and $\delta^{13}C_{wax}$ values for each species and applies a Bayesian framework to estimate the fractional contribution of each source (i.e., BLB plants) to a mixture (i.e., BLB sediments).

This model does not take into account interspecies differences in wax concentrations or molecular distributions, and therefore offers a simplified analysis of this system. Nevertheless, we used this model as a tool to explore the δ^2H_{wax} and $\delta^{13}C_{wax}$ data from BLB and found that, for *n*-C_{29} alkane, the species with the greatest fractional contribution to bog sediments were *Q. rubra* (0.59) and *V. macrocarpon* (0.24), with smaller contributions from *P. serotina* (0.028) and *T. vernix* (0.026; Supplementary Table S3; Supplementary Fig. S1). This includes the tree species that produce the highest abundance of long-chain *n*-alkanes (*Q. rubra* and *P. serotina*) and one of the two dominant shrubs in the bog shoreline zone (*T. vernix*). The woody groundcover species *V. macrocarpon* had a relatively large modeled contribution, perhaps because its exceptionally ^2H-depleted *n*-C_{29} alkane value (−229‰; Tables 1 and 3) was necessary to bring a mainly tree-derived δ^2H_{wax} signal in line with values in sediments (Fig. 6, Supplementary Table S1). This is an interesting result in that, even though the simmr model

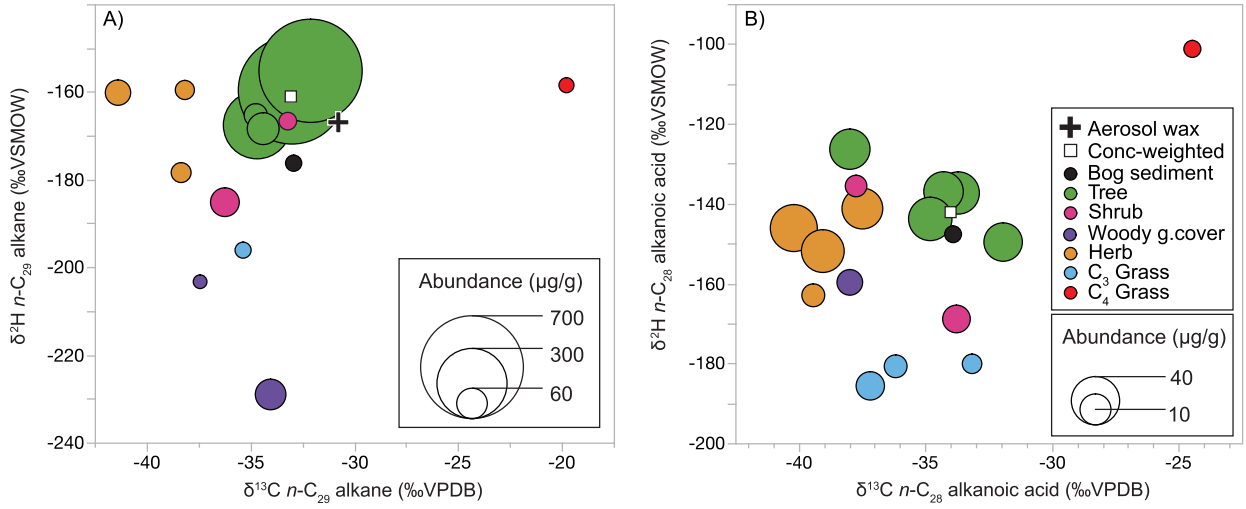

Fig. 6. Plots of the δ^2H and $\delta^{13}C$ values of: (A) *n*-C_{29} alkane and (B) *n*-C_{28} alkanoic acid in sediments and plant growth forms at BLB. Each point represents mean isotope values for a different species, based on data from replicate individuals sampled from each species. The size of each point is scaled to the lipid concentration in µg/g dry leaf or dry sediment, with different point size scales inset in panels A and B. Points are color coded by growth form. Points representing bog sediments are black. Concentration-weighted isotope values for all source vegetation are plotted as open squares. The isotopic composition of pooled rain-scavenged aerosol *n*-alkanes is indicated with a cross in panel A.

does not include concentration data, the strong influence of trees that produce the most wax was apparent in the model results on the basis of δ^2H and $\delta^{13}C$ values alone.

It is notable in that all of the species with a high modeled contribution to sediments were woody, but include three different growth forms (trees, shrubs and woody groundcover). This suggests the dominance of trees, modified by woody plant sources in close proximity to the basin regardless of growth form or species-dependent plant wax concentration. This is consistent with molecular and isotopic evidence from prior source apportionment studies that trees were a dominant source of sedimentary lipids (Sachse et al., 2004; Seki et al., 2010; Tipple and Pagani, 2013; Cooper et al., 2015).

Weighting the $\varepsilon_{n\text{-C29/MAP}}$ values of each species by the simmr model estimates of the fractional contribution of each species gives an overall $\varepsilon_{n\text{-C29/MAP}}$ of −132‰ and yields a δ^2H_{MAP} of −50‰ for BLB when applied to sedimentary n-C_{29} alkane δ^2H values (Supplementary Table S3). This is identical to both the OIPC-modeled δ^2H_{MAP} (Welker, 2000; Bowen and Revenaugh, 2003; IAEA/WMO, 2015; Bowen, 2017) and mean δ^2H_{xw} across the 2014 growing season (Freimuth et al., 2017). This confirms that, while the modeled proportional contributions are just one possible scenario based only on δ^2H and $\delta^{13}C$ values, the resulting estimates are reasonable and reflect the fidelity of n-alkanes from woody plants as recorders of precipitation.

4.3. Sediment bias toward n-alkanoic acid sources

In contrast to n-alkanes, the concentration-weighted mean n-C_{28} alkanoic acid δ^2H and $\delta^{13}C$ values for all species (−142‰ and −34‰; Fig. 6) are within approximately one standard deviation of the measured mean δ^2H and $\delta^{13}C$ in sediments (−148 ± 5‰ and −33.9 ± 0.4‰, respectively). This likely reflects the more uniform distribution of n-C_{28} alkanoic acid concentrations across growth forms. As with n-C_{29} alkane, the simmr model predicts that trees have the greatest contribution to sedimentary n-C_{28} alkanoic acid (Supplementary Fig. S2; Supplementary Table S3). The four species with the greatest fractional contribution to n-C_{28} alkanoic acid δ^2H values in sediment were all trees: *P. serotina* (0.42), *A. saccharinum* (0.10), *Q. alba* (0.07), and *Q. rubra* (0.06). The modeled fractional contributions from all remaining species showed little variation, ranging from 0.03 to 0.04. If these modeled contributions are accurate, then sedimentary n-C_{28} alkanoic acids may be more strongly biased toward trees than n-C_{29} alkanes, which may be more generally derived from woody trees, shrubs and groundcover. The tree-dominated model results for n-C_{28} alkanoic acid isotopes are consistent with molecular signatures, which suggest that sediment $ACL_{26\text{-}30}$ reflects that of trees more than any other plant source (Figs. 3 and 5).

To assess model estimates, we weighted the measured $\varepsilon_{n\text{-C28/MAP}}$ of each plant species by its modeled contribution to sediments, which yields an overall $\varepsilon_{n\text{-C28/MAP}}$ of −58‰ and a reconstructed δ^2H_{MAP} of −95‰, which differs considerably from the expected δ^2H_{MAP} of −50‰ (Supplementary Table S3). This suggests that the model may in fact overestimate the combined n-C_{28} alkanoic acid contributions from sources other than trees. Using the $\varepsilon_{n\text{-C28/MAP}}$ for trees only (−92‰) yields a δ^2H_{MAP} estimate of −61‰ based on sediment δ^2H_{wax}. When using the $\varepsilon_{n\text{-C28/xw}}$ value for trees, reconstructed δ^2H_{MAP} (−48‰) is much closer to the expected value. Together, these results support that sedimentary n-C_{28} alkanoic acids are weighted toward contributions from trees, but small contributions from other plant sources are possible given the similar n-alkanoic acid concentrations among species and the close agreement between sediment and concentration-weighted plant wax isotope values (Fig. 6).

In summary, at BLB and perhaps other similar closed basins in forested catchments, long-chain n-alkanoic acids and n-alkanes in sediments are mainly a locally derived signal. If the signal were regionally integrated, we would expect to see a more prominent C_4 influence in the sedimentary $\delta^{13}C_{wax}$ values, but this is not the case. Therefore, our data suggest direct leaf fall as a main transport mechanism. This is supported by field observations of intact *Q. rubra* and *P. serotina* leaves among the litter in the shoreline vegetation zone surrounding the bog (see photographs in Supplementary Fig. S3). This is notable because *Q. rubra* growth is restricted to the relatively well-drained kames in the interior of the forest (sampling sites indicated in Fig. 1), located further from the bog than any other sampled plants. This visual evidence indicates wind-blown leaves transported several hundred m as a significant transport mechanism, which is supported by wax isotopic composition in BLB sediments and is consistent with leaf taphonomy literature (see Diefendorf and Freimuth, 2017 for a review on leaf taphonomy).

4.4. Molecular and isotopic differences between n-alkanes and n-alkanoic acids

There were several molecular and isotopic differences between n-alkanes and n-alkanoic acids at BLB that may influence their application as proxies for past δ^2H_p. First, leaf wax concentrations among species varied by two orders of magnitude for n-alkanes but not for n-alkanoic acids (Fig. 3). This is consistent with prior studies that found relatively consistent n-alkanoic acid concentrations among species compared to greater variability in n-alkanes (Diefendorf et al., 2011; Bush and McInerney, 2013; Polissar et al., 2014). The evidence that sedimentary n-alkanoic acids may be more strongly biased toward trees than n-alkanes (which may reflect woody plants more generally) suggests that leaf wax abundance among species or compound classes is not necessarily a direct indicator of the dominant sources to sediments. Given the differences in source water for trees (precipitation-fed soil water) and shoreline plants (^2H-enriched bog water) at BLB, a stronger bias toward trees may make sedimentary n-C_{28} alkanoic acid a higher-fidelity proxy for precipitation δ^2H. By contrast, if sedimentary n-C_{29} alkanes are derived from more varied woody plant sources (trees as well as shoreline shrubs and groundcover), their δ^2H values may reflect more mixed source waters including the bog itself.

Second, we observed a consistent negative offset in n-C_{29} alkane δ^2H values relative to n-C_{28} alkanoic acid, both in plants and in sediments. The offset in plants was variable, ranging from −19‰ (C_3 graminoids) to −61‰ (woody groundcover); however, mean offsets ranged from −26‰ to −23‰ in herbs, trees and shrubs, closely reflecting that in sediments (−27‰). An offset of comparable magnitude and sign has previously been observed in temperate settings and attributed to fractionation associated with biosynthesis of the two compounds (Chikaraishi and Naraoka, 2007; Hou et al., 2007b; Freimuth et al., 2017). Persistence of this offset in sediments may warrant application of different ε_{app} values to each compound in sediment records, especially considering that existing calibrations of ε_{app} in plants have mainly been developed for n-alkanes (e.g., Sachse et al., 2012). For example, applying ε_{app} values based on calibration data from n-alkanes to sedimentary n-alkanoic acids at BLB would overestimate δ^2H_{MAP} by approximately 30‰. However, we note that while systematic δ^2H offsets between compound classes is a common feature in temperate settings dominated by plants with a single annual leaf flush, this may not be a relevant consideration in settings with a higher diversity of plant species and leaf lifespans (Gao et al., 2014a; Feakins et al., 2016).

Lastly, we compared the $\delta^{13}C$ and δ^2H values of n-alkanes and n-alkanoic acids from trees and shrubs at BLB and found a significant

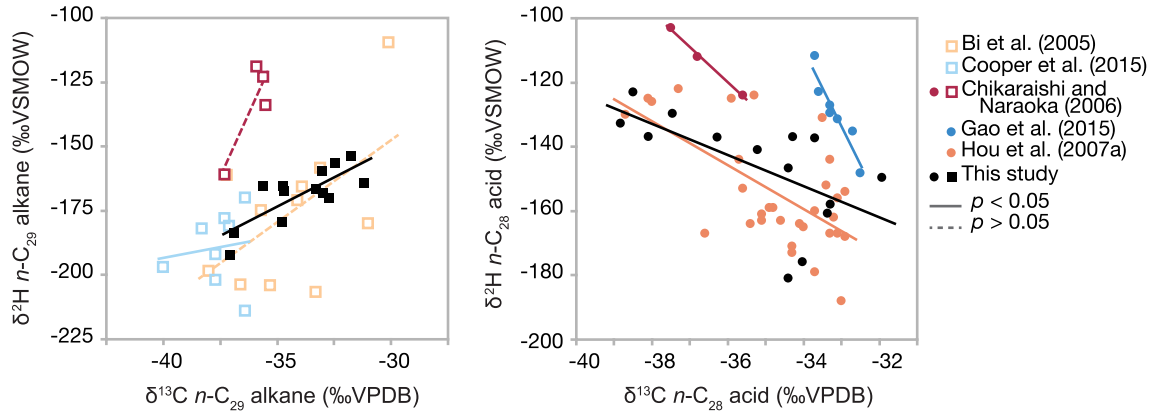

Fig. 7. Regressions of the $\delta^{13}C$ and $\delta^{2}H$ values of n-C_{29} alkanes (squares, left panel) and n-C_{28} alkanoic acids (circles, right panel) from trees and woody shrubs this study (black symbols) and comparable prior studies (colored symbols). Significant regressions ($p < 0.05$) are indicated with filled symbols and solid regression lines. Regressions with $p > 0.05$ are indicated with open symbols and dashed regression lines.

positive correlation for n-C_{29} alkane ($R^2 = 0.61$, $p = 0.0015$) and a significant negative correlation for n-C_{28} alkanoic acid ($R^2 = 0.38$, $p = 0.0182$; Fig. 7). Comparable trends have been reported separately for n-C_{29} alkanes (Bi et al., 2005) and n-C_{28} alkanoic acids (Hou et al., 2007a) from C_3 trees sampled in temperate settings, but it is difficult to assess whether these relationships are robust because relatively few studies have reported both $\delta^{13}C_{wax}$ and $\delta^{2}H_{wax}$ from multiple coexisting tree species, and several of these have not observed a significant relationship (e.g., Chikaraishi and Naraoka, 2007; Cooper et al., 2015; Wu et al., 2017). The negative relationship observed here for n-C_{28} alkanoic acid (Fig. 7) may reflect that plants with higher water use efficiency (WUE), indicated by more positive $\delta^{13}C_{wax}$ values, undergo less transpirational ^{2}H-enrichment of intracellular water and therefore have more negative $\delta^{2}H_{wax}$ values (Hou et al., 2007a). It remains unclear why the sign of this relationship would differ between compound classes, but we speculate that if n-alkanes are produced during the brief period of leaf expansion (Kahmen et al., 2011; Tipple et al., 2013; Oakes and Hren, 2016; Freimuth et al., 2017; Suh and Diefendorf, 2018; Tipple and Ehleringer, 2018) and n-alkanoic acids throughout the entire growing season (Freimuth et al., 2017), then this may reflect contrasting metabolic status, photosynthetic rates, stomatal conductance and WUE during the production of n-alkanes in young, rapidly expanding leaves and n-alkanoic acids in mature, opportunistic leaves. Future studies including the $\delta^{13}C$ and $\delta^{2}H$ composition of multiple wax compound classes could further test these putative relationships and their potential dependence on plant type or growth environment.

Molecular and isotopic evidence suggests that the wax signal recorded in bog sediments is mainly locally derived (e.g., reflecting direct leaf fall from woody catchment vegetation) rather than regionally integrated (e.g., reflecting rain-scavenged aerosol waxes or regionally dominant *Z. mays*). Based on $\delta^{2}H_{wax}$ and $\delta^{13}C_{wax}$, sedimentary n-C_{28} alkanoic acids are primarily tree-derived and may therefore be more reflective of soil water (i.e., precipitation), whereas sedimentary n-C_{29} alkanes are integrated from a mix of trees and woody shoreline plants and may therefore reflect more mixed water sources including bog water. Additionally, in trees and woody shrubs, we observed a negative (positive) correlation between $\delta^{2}H_{wax}$ and $\delta^{13}C_{wax}$ for n-C_{28} alkanoic acids (n-C_{29} alkanes), consistent with limited comparable data. We speculate that $\delta^{2}H_{wax}$–$\delta^{13}C_{wax}$ relationships of opposite sign may reflect contrasting plant metabolic status and WUE during biosynthesis of n-alkanes (during spring leaf expansion) and n-alkanoic acids (throughout the growing season), however this hypothesis is presently supported only for deciduous woody plants in temperate settings and requires further testing.

In sediments, we observed a ~30‰ offset in ε_{app} values for n-C_{29} alkanes (−133‰) and n-C_{28} alkanoic acids (−103‰), a feature previously observed in temperate settings. These findings demonstrate that, while ε_{app} variability is often large (>70‰) at the plant level, sedimentary wax records are strongly biased toward trees and other woody vegetation growing in close proximity to the basin. This can help guide ε_{app} estimates for similar depositional settings (i.e., hydrologically closed basins in forested catchments), especially when the presence and composition of forests can be independently constrained.

5. Conclusions

We surveyed leaf waxes (n-alkanes and n-alkanoic acids) in all major plant species growing in the BLB catchment and compared their concentration, molecular distribution and isotopic composition ($\delta^{2}H$ and $\delta^{13}C$) with that in bog sediments. Sampled species included a range of growth forms occupying the bog shoreline and primarily accessing bog water, as well as trees that dominate forested areas and primarily access precipitation-fed soil water. n-Alkane concentrations were variable among species and were highest in trees, while long-chain n-alkanoic acid concentrations were generally lower and more evenly distributed among growth forms. The total range in sedimentary $\delta^{2}H_{wax}$ (9–11‰) was considerably smaller than in plants at BLB (77–84‰), indicating some integration processes in sediments.

Acknowledgements

We thank Sarah Feakins and one anonymous reviewer for helpful comments that improved this manuscript. The Nature Conservancy granted research access to Brown's Lake Bog State Nature Preserve. Thanks go to Nicholas Wiesenberg, Katherine McNulty and Kelly Grogan for field sampling assistance, and again to Kelly Grogan for laboratory assistance. We thank Erin Mortenson and Daniel Engstrom at the St. Croix Watershed Research Station for sediment ^{210}Pb analysis. This research was supported in part by the US National Science Foundation (EAR-1229114 to AFD and EAR-1636740 to AFD and TVL) and by the Donors of the American Chemical Society Petroleum Research Fund (PRF #51787-DNI2 to AFD). This research was also supported by awards from the Geological Society of America and Sigma Xi to EJF.

Appendix A. Supplementary material

Supplementary data to this article can be found online at https://doi.org/10.1016/j.orggeochem.2019.01.006.

Associate Editor—**Philip Meyers**

References

Aichner, B., Herzschuh, U., Wilkes, H., Vieth, A., Böhner, J., 2010. δD values of *n*-alkanes in Tibetan lake sediments and aquatic macrophytes – a surface sediment study and application to a 16 ka record from Lake Koucha. Organic Geochemistry 41, 779–790.

Bi, X., Sheng, G., Liu, X., Li, C., Fu, J., 2005. Molecular and carbon and hydrogen isotopic composition of *n*-alkanes in plant leaf waxes. Organic Geochemistry 36, 1405–1417.

Bird, B.W., Polisar, P.J., Lei, Y., Thompson, L.G., Yao, T., Finney, B.P., Bain, D.J., Pompeani, D.P., Steinman, B.A., 2014. A Tibetan lake sediment record of Holocene Indian summer monsoon variability. Earth and Planetary Science Letters 399, 92–102.

Bowen, G.J., 2017. The Online Isotopes in Precipitation Calculator, version 3.1. http://www.waterisotopes.org.

Bowen, G.J., Revenaugh, J., 2003. Interpolating the isotopic composition of modern meteoric precipitation. Water Resources Research 39, 1299.

Broddin, G., Cautreels, W., Van Cauwenberghe, K., 1980. On the aliphatic and polyaromatic hydrocarbon levels in urban and background aerosols from Belgium and the Netherlands. Atmospheric Environment 14, 895–910.

Burnham, R.J., Wing, S.L., Parker, G.G., 1992. The reflection of deciduous forest communities in leaf litter; implications for autochthonous litter assemblages from the fossil record. Paleobiology 18, 30–49.

Bush, R.T., McInerney, F.A., 2013. Leaf wax *n*-alkane distributions in and across modern plants: Implications for paleoecology and chemotaxonomy. Geochimica et Cosmochimica Acta 117, 161–179.

Chikaraishi, Y., Naraoka, H., Poulson, S.R., 2004. Hydrogen and carbon isotopic fractionations of lipid biosynthesis among terrestrial (C_3, C_4 and CAM) and aquatic plants. Phytochemistry 65, 1369–1381.

Chikaraishi, Y., Naraoka, H., 2007. $\delta^{13}C$ and δD relationships among three *n*-alkyl compound classes (*n*-alkanoic acid, *n*-alkane and *n*-alkanol) of terrestrial higher plants. Organic Geochemistry 38, 198–215.

Collins, J.A., Schefuß, E., Mulitza, S., Prange, M., Werner, M., Tharammal, T., Paul, A., Wefer, G., 2013. Estimating the hydrogen isotopic composition of past precipitation using leaf-waxes from western Africa. Quaternary Science Reviews 65, 88–101.

Collister, J.W., Rieley, G., Stern, B., Eglinton, G., Fry, B., 1994. Compound-specific $\delta^{13}C$ analyses of leaf lipids from plants with differing carbon dioxide metabolisms. Organic Geochemistry 21, 619–627.

Conte, M.H., Weber, J.C., 2002. Long-range atmospheric transport of terrestrial biomarkers to the western North Atlantic. Global Biogeochemical Cycles 16, 1142.

Conte, M., Weber, J., Carlson, P., Flanagan, L., 2003. Molecular and carbon isotopic composition of leaf wax in vegetation and aerosols in a northern prairie ecosystem. Oecologia 135, 67–77.

Cooper, R.J., Krueger, T., Hiscock, K.M., Rawlins, B.G., 2015. High-temporal resolution fluvial sediment source fingerprinting with uncertainty: a Bayesian approach. Earth Surface Processes and Landforms 40, 78–92.

Coplen, T.B., Brand, W.A., Gehre, M., Gröning, M., Meijer, H.A.J., Toman, B., Verkouteren, R.M., 2006. New guidelines for $\delta^{13}C$ measurements. Analytical Chemistry 78, 2439–2441.

Cranwell, P.A., 1981. Diagenesis of free and bound lipids in terrestrial detritus deposited in a lacustrine sediment. Organic Geochemistry 3, 79–89.

Daniels, W.C., Russell, J.M., Giblin, A.E., Welker, J.M., Klein, E.S., Huang, Y., 2017. Hydrogen isotope fractionation in leaf waxes in the Alaskan Arctic tundra. Geochimica et Cosmochimica Acta 213, 216–236.

Diefendorf, A.F., Mueller, K.E., Wing, S.L., Koch, P.L., Freeman, K.H., 2010. Global patterns in leaf ^{13}C discrimination and implications for studies of past and future climate. Proceedings of the National Academy of Sciences of the United States of America 107, 5738–5743.

Diefendorf, A.F., Freeman, K.H., Wing, S.L., Graham, H.V., 2011. Production of *n*-alkyl lipids in living plants and implications for the geologic past. Geochimica et Cosmochimica Acta 75, 7472–7485.

Diefendorf, A.F., Sberna, D.T., Taylor, D.W., 2015. Effect of thermal maturation on plant-derived terpenoids and leaf wax *n*-alkyl components. Organic Geochemistry 89, 61–70.

Diefendorf, A.F., Freimuth, E.J., 2017. Extracting the most from terrestrial plant-derived *n*-alkyl lipids and their carbon isotopes from the sedimentary record: a review. Organic Geochemistry 103, 1–21.

Doskey, P.V., 2000. The air–water exchange of C_{15}–C_{31} *n*-alkanes in a precipitation-dominated seepage lake. Atmospheric Environment 34, 3981–3993.

Eglinton, G., Hamilton, R.J., 1967. Leaf epicuticular waxes. Science 156, 1322–1335.

Eley, Y., Dawson, L., Black, S., Andrews, J., Pedentchouk, N., 2014. Understanding $^{2}H/^{1}H$ systematics of leaf wax *n*-alkanes in coastal plants at Stiffkey saltmarsh, Norfolk, UK. Geochimica et Cosmochimica Acta 128, 13–28.

Eley, Y., Dawson, L., Pedentchouk, N., 2016. Investigating the carbon isotope composition and leaf wax *n*-alkane concentration of C_3 and C_4 plants in Stiffkey saltmarsh, Norfolk, UK. Organic Geochemistry 96, 28–42.

Feakins, S.J., Sessions, A.L., 2010. Controls on the D/H ratios of plant leaf waxes from an arid ecosystem. Geochimica et Cosmochimica Acta 74, 2128–2141.

Feakins, S.J., Kirby, M.E., Cheetham, M.I., Ibarra, Y., Zimmerman, S.R.H., 2014. Fluctuation in leaf wax D/H ratio from a southern California lake records significant variability in isotopes in precipitation during the late Holocene. Organic Geochemistry 66, 48–59.

Feakins, S.J., Bentley, L.P., Salinas, N., Shenkin, A., Blonder, B., Goldsmith, G.R., Ponton, C., Arvin, L.J., Wu, M.S., Peters, T., 2016. Plant leaf wax biomarkers capture gradients in hydrogen isotopes of precipitation from the Andes and Amazon. Geochimica et Cosmochimica Acta 182, 155–172.

Feakins, S.J., Wu, M.S., Ponton, C., Galy, V., West, A.J., 2018. Dual isotope evidence for sedimentary integration of plant wax biomarkers across an Andes-Amazon elevation transect. Geochimica et Cosmochimica Acta 242, 64–81.

Ficken, K.J., Li, B., Swain, D.L., Eglinton, G., 2000. An *n*-alkane proxy for the sedimentary input of submerged/floating freshwater aquatic macrophytes. Organic Geochemistry 31, 745–749.

Freeman, K.H., Pancost, R.D., 2014. Biomarkers for terrestrial plants and climate. In: Turekian, H.D., Holland, K.K. (Eds.), Treatise on Geochemistry. second ed. Elsevier, pp. 395–416.

Freimuth, E.J., Diefendorf, A.F., Lowell, T.V., 2017. Hydrogen isotopes of *n*-alkanes and *n*-alkanoic acids as tracers of precipitation in a temperate forest and implications for paleorecords. Geochimica et Cosmochimica Acta 206, 166–183.

Gagosian, R.B., Peltzer, E.T., 1986. The importance of atmospheric input of terrestrial organic material to deep sea sediments. Organic Geochemistry 10, 661–669.

Gao, L., Edwards, E.J., Zeng, Y., Huang, Y., 2014a. Major evolutionary trends in hydrogen isotope fractionation of vascular plant leaf waxes. PLoS ONE 9, e112610.

Gao, L., Zheng, M., Fraser, M., Huang, Y., 2014b. Comparable hydrogen isotopic fractionation of plant leaf wax *n*-alkanoic acids in arid and humid subtropical ecosystems. Geochemistry, Geophysics, Geosystems 15, 361–373.

Garcin, Y., Schefuß, E., Schwab, V.F., Garreta, V., Gleixner, G., Vincens, A., Todou, G., Séné, O., Onana, J.-M., Achoundong, G., Sachse, D., 2014. Reconstructing C_3 and C_4 vegetation cover using *n*-alkane carbon isotope ratios in recent lake sediments from Cameroon, Western Central Africa. Geochimica et Cosmochimica Acta 142, 482–500.

Giri, S.J., Diefendorf, A.F., Lowell, T.V., 2015. Origin and sedimentary fate of plant-derived terpenoids in a small river catchment and implications for terpenoids as quantitative paleovegetation proxies. Organic Geochemistry 82, 22–32.

Glover, K.C., Lowell, T.V., Wiles, G.C., Pair, D., Applegate, P., Hajdas, I., 2011. Deglaciation, basin formation and post-glacial climate change from a regional network of sediment core sites in Ohio and eastern Indiana. Quaternary Research 76, 401–410.

Heiri, O., Lotter, A.F., Lemcke, G., 2001. Loss on ignition as a method for estimating organic and carbonate content in sediments: reproducibility and comparability of results. Journal of Paleolimnology 25, 101–110.

Hou, J., D'Andrea, W.J., MacDonald, D., Huang, Y., 2007a. Evidence for water use efficiency as an important factor in determining the δD values of tree leaf waxes. Organic Geochemistry 38, 1251–1255.

Hou, J.Z., D'Andrea, W.J., MacDonald, D., Huang, Y.S., 2007b. Hydrogen isotopic variability in leaf waxes among terrestrial and aquatic plants around Blood Pond, Massachusetts (USA). Organic Geochemistry 38, 977–984.

Hou, J., D'Andrea, W.J., Huang, Y., 2008. Can sedimentary leaf waxes record D/H ratios of continental precipitation? Field, model, and experimental assessments. Geochimica et Cosmochimica Acta 72, 3503–3517.

Huang, Y., Eglinton, G., Ineson, P., Latter, P.M., Bol, R., Harkness, D.D., 1997. Absence of carbon isotope fractionation of individual *n*-alkanes in a 23 year field decomposition experiment with *Calluna vulgaris*. Organic Geochemistry 26, 497–501.

IAEA/WMO, 2015. Global Network of Isotopes in Precipitation. The GNIP Database. https://nucleus.iaea.org/wiser.

Jacob, J., Huang, Y., Disnar, J.-R., Sifeddine, A., Boussafir, M., Albuquerque, A.L.S., Turcq, B., 2007. Paleohydrological changes during the last deglaciation in Northern Brazil. Quaternary Science Reviews 26, 1004–1015.

Kahmen, A., Dawson, T.E., Vieth, A., Sachse, D., 2011. Leaf wax *n*-alkane δD values are determined early in the ontogeny of *Populus trichocarpa* leaves when grown under controlled environmental conditions. Plant, Cell & Environment 34, 1639–1651.

Kahmen, A., Hoffmann, B., Schefuß, E., Arndt, S.K., Cernusak, L.A., West, J.B., Sachse, D., 2013a. Leaf water deuterium enrichment shapes leaf wax *n*-alkane δD values of angiosperm plants II: Observational evidence and global implications. Geochimica et Cosmochimica Acta 111, 50–63.

Kahmen, A., Schefuß, E., Sachse, D., 2013b. Leaf water deuterium enrichment shapes leaf wax *n*-alkane δD values of angiosperm plants I: Experimental evidence and mechanistic insights. Geochimica et Cosmochimica Acta 111, 39–49.

Liu, W., Yang, H., Li, L., 2006. Hydrogen isotopic compositions of *n*-alkanes from terrestrial plants correlate with their ecological life forms. Oecologia 150, 330–338.

Lutz, B., Wiles, G., Lowell, T., Michaels, J., 2007. The 8.2-ka abrupt climate change event in Brown's Lake, northeast Ohio. Quaternary Research 67, 292–296.

McInerney, F.A., Helliker, B.R., Freeman, K.H., 2011. Hydrogen isotope ratios of leaf wax *n*-alkanes in grasses are insensitive to transpiration. Geochimica et Cosmochimica Acta 75, 541–554.

Meyers, P.A., Bourbonniere, R.A., Takeuchi, N., 1980. Hydrocarbons and fatty acids in two cores of Lake Huron sediments. Geochimica et Cosmochimica Acta 44, 1215–1221.
Meyers, P.A., Hites, R.A., 1982. Extractable organic compounds in midwest rain and snow. Atmospheric Environment 16, 2169–2175.
Meyers, P.A., Ishiwatari, R., 1993. Lacustrine organic geochemistry—an overview of indicators of organic matter sources and diagenesis in lake sediments. Organic Geochemistry 20, 867–900.
Nelson, D.B., Knohl, A., Sachse, D., Schefuß, E., Kahmen, A., 2017. Sources and abundances of leaf waxes in aerosols in central Europe. Geochimica et Cosmochimica Acta 198, 299–314.
Nelson, D.B., Ladd, S.N., Schubert, C.J., Kahmen, A., 2018. Rapid atmospheric transport and large-scale deposition of recently synthesized plant waxes. Geochimica et Cosmochimica Acta 222, 599–617.
Newberry, S.L., Kahmen, A., Dennis, P., Grant, A., 2015. *n*-Alkane biosynthetic hydrogen isotope fractionation is not constant throughout the growing season in the riparian tree *Salix viminalis*. Geochimica et Cosmochimica Acta 165, 75–85.
Nguyen Tu, T.T., Egasse, C., Anquetil, C., Zanetti, F., Zeller, B., Huon, S., Derenne, S., 2017. Leaf lipid degradation in soils and surface sediments: a litterbag experiment. Organic Geochemistry 104, 35–41.
Nichols, J., Booth, R.K., Jackson, S.T., Pendall, E.G., Huang, Y., 2010. Differential hydrogen isotopic ratios of *Sphagnum* and vascular plant biomarkers in ombrotrophic peatlands as a quantitative proxy for precipitation—evaporation balance. Geochimica et Cosmochimica Acta 74, 1407–1416.
Oakes, A.M., Hren, M.T., 2016. Temporal variations in the δD of leaf *n*-alkanes from four riparian plant species. Organic Geochemistry 97, 122–130.
Pagani, M., Pedentchouk, N., Huber, M., Sluijs, A., Schouten, S., Brinkhuis, H., Sinninghe Damsté, J.S., Dickens, G.R.Expedition 302 Scientists, 2006. Arctic hydrology during global warming at the Palaeocene/Eocene thermal maximum. Nature 442, 671–675.
Pancost, R.D., Boot, C.S., 2004. The palaeoclimatic utility of terrestrial biomarkers in marine sediments. Marine Chemistry 92, 239–261.
Parnell, A.C., Inger, R., Bearhop, S., Jackson, A.L., 2010. Source partitioning using stable isotopes: coping with too much variation. PLoS ONE 5, e9672.
Parnell, A.C., Phillips, D.L., Bearhop, S., Semmens, B.X., Ward, E.J., Moore, J.W., Jackson, A.L., Grey, J., Kelly, D.J., Inger, R., 2013. Bayesian stable isotope mixing models. Environmetrics 24, 387–399.
Parnell, A., 2016. simmr: A Stable Isotope Mixing Model. R package version 0.3. https://CRAN.R-project.org/package=simmr.
Pedentchouk, N., Sumner, W., Tipple, B., Pagani, M., 2008. $\delta^{13}C$ and δD compositions of *n*-alkanes from modern angiosperms and conifers: an experimental set up in central Washington State, USA. Organic Geochemistry 39, 1066–1071.
Polissar, P., Preefer, M., Liu, C., 2014. Fidelity of leaf-wax *n*-alkane and n-alkanoic acid D/H ratios in space and time. American Geophysical Union Fall Meeting, PP43E-07.
Polissar, P.J., Freeman, K.H., 2010. Effects of aridity and vegetation on plant-wax δD in modern lake sediments. Geochimica et Cosmochimica Acta 74, 5785–5797.
R Core Team, 2017. R: A language and environment for statistical computing. R Foundation for Statistical Computing, Vienna, Austria. https://www.R-project.org/.
Rach, O., Brauer, A., Wilkes, H., Sachse, D., 2014. Delayed hydrological response to Greenland cooling at the onset of the Younger Dryas in western Europe. Nature Geoscience 7, 109–112.
Rommerskirchen, F., Plader, A., Eglinton, G., Chikaraishi, Y., Rullkötter, J., 2006. Chemotaxonomic significance of distribution and stable carbon isotopic composition of long-chain alkanes and alkan-1-ols in C_4 grass waxes. Organic Geochemistry 37, 1303–1332.
Sachse, D., Radke, J., Gleixner, G., 2004. Hydrogen isotope ratios of recent lacustrine sedimentary *n*-alkanes record modern climate variability. Geochimica et Cosmochimica Acta 68, 4877–4889.
Sachse, D., Radke, J., Gleixner, G., 2006. δD values of individual *n*-alkanes from terrestrial plants along a climatic gradient – implications for the sedimentary biomarker record. Organic Geochemistry 37, 469–483.
Sachse, D., Kahmen, A., Gleixner, G., 2009. Significant seasonal variation in the hydrogen isotopic composition of leaf-wax lipids for two deciduous tree ecosystems (*Fagus sylvativa* and *Acer pseudoplatanus*). Organic Geochemistry 40, 732–742.
Sachse, D., Gleixner, G., Wilkes, H., Kahmen, A., 2010. Leaf wax *n*-alkane δD values of field-grown barley reflect leaf water δD values at the time of leaf formation. Geochimica et Cosmochimica Acta 74, 6741–6750.
Sachse, D., Billault, I., Bowen, G.J., Chikaraishi, Y., Dawson, T.E., Feakins, S.J., Freeman, K.H., Magill, C.R., McInerney, F.A., van der Meer, M.T.J., Polissar, P., Robins, R.J., Sachs, J.P., Schmidt, H.-L., Sessions, A.L., White, J.W.C., West, J.B., Kahmen, A., 2012. Molecular paleohydrology: Interpreting the hydrogen-isotopic composition of lipid biomarkers from photosynthesizing organisms. Annual Review of Earth Planetary Sciences 40, 221–249.
Schimmelmann, A., Sessions, A.L., Mastalerz, M., 2006. Hydrogen isotopic (D/H) composition of organic matter during diagenesis and thermal maturation. Annual Review of Earth Planetary Sciences 34, 501–533.
Sanger, J.E., Crowl, G.H., 1979. Fossil pigments as a guide to the paleolimnology of Browns Lake, Ohio. Quaternary Research 11, 342–352.
Seki, O., Nakatsuka, T., Shibata, H., Kawamura, K., 2010. A compound-specific *n*-alkane $\delta^{13}C$ and δD approach for assessing source and delivery processes of terrestrial organic matter within a forested watershed in northern Japan. Geochimica et Cosmochimica Acta 74, 599–613.
Sessions, A.L., Sylva, S.P., Summons, R.E., Hayes, J.M., 2004. Isotopic exchange of carbon-bound hydrogen over geologic timescales. Geochimica et Cosmochimica Acta 68, 1545–1559.
Sessions, A.L., 2016. Factors controlling the deuterium contents of sedimentary hydrocarbons. Organic Geochemistry 96, 43–64.
Simoneit, B.R.T., Chester, R., Eglinton, G., 1977. Biogenic lipids in particulates from lower atmosphere over eastern Atlantic. Nature 267, 682–685.
Smith, F.A., Freeman, K.H., 2006. Influence of physiology and climate on δD of leaf wax *n*-alkanes from C_3 and C_4 grasses. Geochimica et Cosmochimica Acta 70, 1172–1187.
Suh, Y.J., Diefendorf, A.F., 2018. Seasonal and canopy height variation in *n*-alkanes and their carbon isotopes in a temperate forest. Organic Geochemistry 116, 23–34.
Tierney, J.E., Russell, J.M., Huang, Y., Sinninghe Damsté, J.S., Hopmans, E.C., Cohen, A.S., 2008. Northern hemisphere controls on tropical southeast African climate during the past 60,000 years. Science 322, 252–255.
Tierney, J.E., Pausata, F.S.R., deMenocal, P.B., 2017. Rainfall regimes of the Green Sahara. Science Advances 3, e1601503.
Tipple, B.J., Berke, M.A., Doman, C.E., Khachaturyan, S., Ehleringer, J.R., 2013. Leaf-wax *n*-alkanes record the plant–water environment at leaf flush. Proceedings of the National Academy of Sciences of the United States of America 110, 2659–2664.
Tipple, B.J., Pagani, M., 2013. Environmental control on eastern broadleaf forest species' leaf wax distributions and D/H ratios. Geochimica et Cosmochimica Acta 111, 64–77.
Tipple, B.J., Ehleringer, J.R., 2018. Distinctions in heterotrophic and autotrophic-based metabolism as recorded in the hydrogen and carbon isotope ratios of normal alkanes. Oecologia 187, 1053–1075.
van Bree, L.G.J., Peterse, F., van der Meer, M.T.J., Middelburg, J.J., Negash, A.M.D., De Crop, W., Cocquyt, C., Wieringa, J.J., Verschuren, D., Sinninghe Damsté, J.S., 2018. Seasonal variability in the abundance and stable carbon-isotopic composition of lipid biomarkers in suspended particulate matter from a stratified equatorial lake (Lake Chala, Kenya/Tanzania): implications for the sedimentary record. Quaternary Science Reviews 192, 208–224.
Welker, J., 2000. Isotopic ($\delta^{18}O$) characteristics of weekly precipitation collected across the USA: an initial analysis with application to water source studies. Hydrological Processes 14, 1449–1464.
West, A.G., Patrickson, S.J., Ehleringer, J.R., 2006. Water extraction times for plant and soil materials used in stable isotope analysis. Rapid Communications in Mass Spectrometry 20, 1317–1321.
Wu, M.S., Feakins, S.J., Martin, R.E., Shenkin, A., Bentley, L.P., Blonder, B., Salinas, N., Asner, G.P., Malhi, Y., 2017. Altitude effect on leaf wax carbon isotopic composition in humid tropical forests. Geochimica et Cosmochimica Acta 206, 1–17.
Yang, H., Huang, Y., 2003. Preservation of lipid hydrogen isotope ratios in Miocene lacustrine sediments and plant fossils at Clarkia, northern Idaho, USA. Organic Geochemistry 34, 413–423.